DELFT UNIVERSITY OF TECHNOLOGY

REPORT 15-03

Numerical stability for velocity-based 2-phase formulation for geotechnical dynamic analysis

M.M.J. Mieremet

ISSN 1389-6520

Reports of the Delft Institute of Applied Mathematics

Delft 2015

PREFACE

As a master student in Applied Mathematics at the Delft University of Technology I am highly educated in Numerical Analysis. My interest in this field even made me choose elective courses such as Advanced Numerical Methods, Applied Finite Elements and Computational Fluid Dynamics. In my search for a challenging graduation project I chose a research proposal on the material point method, an extension of the finite element method that is well-suited for problems involving large deformations. The proposal met al my personal requirements, since it contained a mathematical basis I am already familiar with and the opportunity to gain knowledge about a relatively new numerical method. Furthermore, it included an internship at Deltares.

I would like to thank Professor Cees Vuik from Delft University of Technology for supporting this choice and Dr. Lars Beuth from Deltares for giving me the chance to work on this project. I also wish to thank Professor Stolle from McMaster University and Francesca Ceccato from University of Padua. Both have supported me during this preliminary study and I hope they keep on supporting me during the rest of my thesis. Finally, I may not forget my direct colleagues at Deltares for providing a nice working environment.

M.M.J. Mieremet
Delft, April 2015

CONTENTS

INTRODUCTION

The demand for safe, sustainable and cost-efficient engineering solutions, the need to tackle new complex technological challenges or simply the desire for daring new designs motivate extensive efforts worldwide in research and development of numerical methods for engineering applications such as the widely-used finite element method (FEM). Inversely, progress in numerical methods opens new possibilities for engineers to explore innovative approaches in problem-solving or product design.
One may think of numerical simulations of oil drilling on the ocean floor or analyses related to construction works such as the Eastern Scheldt storm surge barrier [1] or the Amsterdam Metro North-South Line [2], both in the Netherlands. Such works are of high relevance for society or, at least, generally involve considerable investments. High importance may therefore be attributed to the ability to accurately predict the mechanical behaviour of soil under various circumstances by means of numerical methods. This is certainly a demanding task and requires the accurate physical modeling of soil.

Soil is a porous medium, a more or less dense agglomeration of grains of different shapes and sizes. Its pore volume is filled with a liquid and/or gas as illustrated in Figure 1. Its mechanical behaviour is certainly no less complex than that of biological tissues or modern high-tech materials used in aircrafts that are likewise the subject of extensive research.

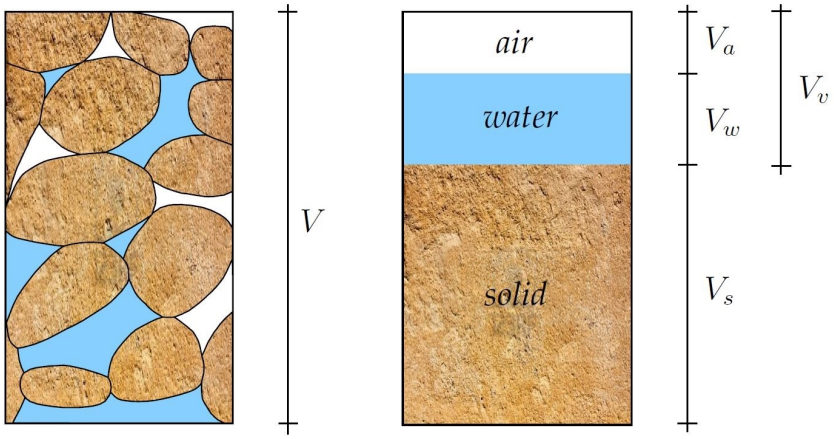

Figure 1: Constituents of soil: solid, liquid and gas phase [3]

Consider for example the common situation of water-saturated soil with a low permeability, e.g. clay. Upon loading pore water slowly dissipates out of the soil. As the pore water flows out of the soil the load is transferred gradually from the pore water to the compacting 'skeleton' of soil grains. In geotechnical engineering this phenomenon is called consolidation. A physical model which describes this phenomenon was first developed by Terzaghi [4] and Biot [5]. Here, water-saturated soil is considered as a 2-phase material, i.e. a material consisting of a solid and liquid constituent. The gas phase is neglected as commonly done in geotechnical engineering.

Subject of this thesis is to improve the stability of finite element analyses of three dimensional dynamic consolidation processes. In this study a velocity-based 2-phase formulation developed by Van Esch, Stolle and Jassim [6] based on Verruijt [7] is considered. In this formulation, the porous medium is modeled as a homogeneous and isotropic continuum. A continuum implies that the medium is continuously distributed across the domain it covers. Homogeneous and isotropic mean that the continuum has the same material properties at any material point and in any direction.

The 2-phase formulation has been implemented by the above-mentioned authors using the Euler-Cromer time integration scheme. This semi-implicit scheme is conditionally stable which means that the time step size in which numerical integration is performed is limited.
Currently the critical time step is estimated by the well-known stability criterion for 1-phase computations. However, when Ceccato performed numerical analyses with the 2-phase formulation considering soil with a low permeability, she encountered a numerical instability [8] as the 1-phase criterion does not apply to partially drained conditions. Results indicated a dependence of the time step on the permeability. The aim of this thesis is to find the missing stability criterion.
Obtaining such a criterion will increase the efficiency of numerical analyses with the considered 2-phase formulation, by replacing rough estimates of the time step size. In case of computations with more than 100,000 time steps the difference in computation time might be significant.

At Deltares, which supported this thesis, a material point method is being developed for large deformation analyses of geotechnical problems. Due to its similarity with FEM, results are expected to be directly transferable to this method.
Since the velocity-based 2-phase formulation is valid for saturated porous media in general, the benefit of this work is not limited to geotechnical problems, but is also of use in solving problems involving other porous materials e.g. biological tissues, ceramics and sponges.

In order to tackle this challenging task a step by step approach is taken. This preliminary study considers only the discretization of a one dimensional small deformation problem involving a linear-elastic material. At first, a 1-phase formulation considering drained conditions is treated. Afterwards, the study is extended to a simplified 2-phase formulation proposed by Stolle (personal communication, 2014). The full 2-phase formulation in both one and three dimensions will be addressed later.

The content of this report follows the approach taken. In Chapter 1 the physical model is described for 1-phase materials. Then the space and time discretization are treated in Chapters 2 and 3, respectively. The stability analysis is presented in Chapter 4 considering the Von Neumann and matrix method. To confirm the correctness of the study, validation of the criterion is presented in Chapter 5.
In the second part of the study the liquid phase is introduced. A simplified 2-phase formulation is given in Chapter 6, followed by its space and time discretization in Chapter 7 and 8, respectively. Chapter 9 treats the stability analyses and presents the obtained stability criteria. The stability criteria are validated in Chapter 10. Finally, some concluding remarks on this study are presented, as well as recommendations for future work.

PART I

CONSIDERATION OF SOIL AS A 1-PHASE CONTINUUM

1

PHYSICAL MODEL

This chapter introduces a three dimensional physical model for small deformations of a 1-phase continuum. First the relevant differential equations are introduced in Section 1.1 including the definitions of variables and parameters. Initial and boundary conditions are explained in detail in Section 1.2. A stability analysis of a three dimensional formulation is however very complex. For that reason the physical model is applied to a one dimensional problem in Section 1.3. It introduces the oedometer test as the leading problem of the following chapters. It is proposed to address the stability analysis of the three dimensional case at a later stage of this thesis.

1.1. EQUATIONS

The original shape of a solid at time t_0 is in the following called the initial configuration $\Omega_0 \in \mathbb{R}^3$ with boundary $\partial\Omega_0$. After a certain deformation it has changed into a configuration $\Omega \in \mathbb{R}^3$ with boundary $\partial\Omega$ at time $t > t_0$ (see Figure 1.1). This relation can be stated pointwise. For this we consider the initial position $\mathbf{x}_0$ and the updated position $\mathbf{x}$ of a particle, which are related by some function

$$\mathbf{x} = \mathbf{x}(\mathbf{x}_0, t). \tag{1.1}$$

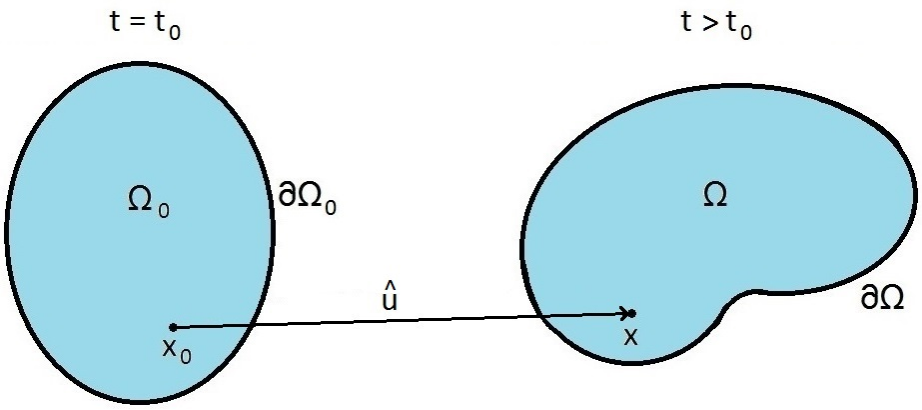

Figure 1.1: Initial and deformed configuration

The positive Cartesian coordinate system is chosen as a frame of reference since it is used for the problems considered in this thesis. This means that each vector consists of three components

$$\mathbf{x}_0 = \begin{bmatrix} x_{01} & x_{02} & x_{03} \end{bmatrix}^T \quad \text{and} \quad \mathbf{x} = \begin{bmatrix} x_1 & x_2 & x_3 \end{bmatrix}^T, \tag{1.2}$$

where the x_1-x_2 plane is said to be horizontal and the x_3-axis represents the vertical direction.

When dealing with deformations it is more convenient to look at the displacement of the material

$$\hat{\mathbf{u}}(\mathbf{x}_0, t) = \begin{bmatrix} \hat{u}_1 & \hat{u}_2 & \hat{u}_3 \end{bmatrix}^T \tag{1.3}$$

which is the difference between the updated position $\mathbf{x}$ and the initial position $\mathbf{x}_0$

$$\hat{\mathbf{u}}(\mathbf{x}_0, t) = \mathbf{x}(\mathbf{x}_0, t) - \mathbf{x}_0. \tag{1.4}$$

The velocity of the solid is related to the displacement by differentiation. In the Eulerian description the total derivative is considered, while in the Lagrangian description the partial derivative is considered. The reason for this difference is the fact that in the Lagrangian description the convective term of the total derivative vanishes [9]. Since in this study the Lagrangian description is considered, the velocity is related to the displacement by

$$\hat{\mathbf{v}}(\mathbf{x}_0, t) = \frac{\partial \hat{\mathbf{u}}}{\partial t}(\mathbf{x}_0, t). \tag{1.5}$$

Without further notice we present partial derivatives wherever necessary in this study.

From the velocity the strain rate and rotation rate tensors are derived. The strain rate tensor describes the 'rate of deformation' with respect to the initial configuration and equals the symmetric part of the velocity gradient tensor

$$\frac{\partial \hat{\varepsilon}_{ij}}{\partial t} = \frac{1}{2}\left(\frac{\partial \hat{v}_i}{\partial x_{0j}} + \frac{\partial \hat{v}_j}{\partial x_{0i}}\right). \tag{1.6}$$

The rotation rate tensor on the other hand describes the 'rate of rotation' with respect to the initial configuration and equals the antisymmetric part of the velocity gradient tensor

$$\frac{\partial \hat{\omega}_{ij}}{\partial t} = \frac{1}{2}\left(\frac{\partial \hat{v}_i}{\partial x_{0j}} - \frac{\partial \hat{v}_j}{\partial x_{0i}}\right). \tag{1.7}$$

The nine components of the stress tensor represent the forces that neighboring particles of the continuum exert on each other in an average sense and can be assembled in a (symmetrical) 3-by-3 matrix

$$\hat{\sigma}_{ij} = \begin{bmatrix} \hat{\sigma}_{11} & \hat{\sigma}_{12} & \hat{\sigma}_{13} \\ \hat{\sigma}_{21} & \hat{\sigma}_{22} & \hat{\sigma}_{23} \\ \hat{\sigma}_{31} & \hat{\sigma}_{32} & \hat{\sigma}_{33} \end{bmatrix}. \tag{1.8}$$

The diagonal entries represent the normal stress and the off-diagonal entries the shear stress, see Figure 1.2. A positive value is consistent with tension.

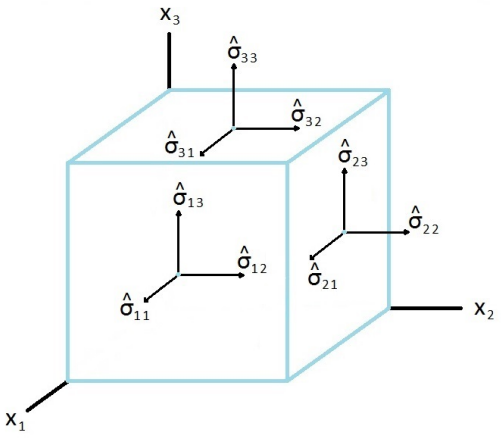

Figure 1.2: Visualization of the stress tensor $\hat{\sigma}_{ij}$ in the Cartesian coordinate system

Stress and strain are related to each other by a constitutive relation. Taking into account the generally non-linear behaviour of soil this constitutive relation can be very complex and can depend on a large number of material parameters. Geometric non-linearity might require consideration as well in the stress-strain relation when deformations become large, i.e. exceeding a length change of about 5 per cent.

In this study small deformations are considered which render the following constitutive relation

$$\frac{\partial \hat{\sigma}_{ij}}{\partial t} = D_{ijkl}\frac{\partial \hat{\varepsilon}_{kl}}{\partial t}. \tag{1.9}$$

For an isotropic linear elastic material the constants D_{ijkl} are defined to be

$$D_{ijkl} = \left(K - \frac{2}{3}G\right)\delta_{ij}\delta_{kl} + G\left(\delta_{ik}\delta_{jl} + \delta_{il}\delta_{jk}\right), \tag{1.10}$$

with δ_{ij} the Kronecker delta. The parameters K and G refer to the bulk modulus and the shear modulus

$$K = \frac{E}{3(1-2\nu)} \quad \text{and} \quad G = \frac{E}{2(1+\nu)}, \tag{1.11}$$

that depend on Young's modulus E and Poisson's ratio ν. They are measures for the stiffness and the absolute ratio between lateral and axial deformation, respectively.

With the constitutive relation we have a relation between the velocity profile and the change of stress. However, the inverse is also possible. The momentum equation describes the change of momentum due to both internal and external forces. The internal forces are described by the stress profile, while we consider gravitational forces as external forces

$$\rho\frac{\partial \hat{v}_i}{\partial t} = \frac{\partial \hat{\sigma}_{ij}}{\partial x_{0j}} - \rho g\delta_{i3}. \tag{1.12}$$

This thesis is not meant to go deeply into the theory of continuum mechanics. For further information the reader is referred to e.g. Malvern [10].

In conclusion, the linear deformation of an isotropic continuum can be described in a closed coupled system of the velocity $\hat{\mathbf{v}}$ and stress tensor $\hat{\boldsymbol{\sigma}}$, depending on the density ρ, gravitational acceleration g, Young's modulus E and Poisson's ratio ν. Since we are interested in the displacement $\hat{\mathbf{u}}$ the relation between velocity and displacement is added to the set of equations, rendering

$$\begin{aligned}
\rho\frac{\partial \hat{v}_i}{\partial t} &= \frac{\partial \hat{\sigma}_{ij}}{\partial x_{0j}} - \rho g\delta_{i3},\\
\frac{\partial \hat{\sigma}_{ij}}{\partial t} &= D_{ijkl}\frac{\partial \hat{\varepsilon}_{kl}}{\partial t},\\
\frac{\partial \hat{u}_i}{\partial t} &= \hat{v}_i.
\end{aligned} \tag{1.13}$$

1.2. INITIAL AND BOUNDARY CONDITIONS

Every partial differential equation needs extra conditions to become uniquely solvable. The kind and number of conditions depend on the order of the various derivatives.

The first order time derivatives in the 1-phase formulation in Equation 1.13 has the consequence that one initial condition for the displacement, velocity and stress is needed:

- Initial displacement $\quad \hat{u}_i(\mathbf{x}_0, 0) = \hat{u}_{0i}(\mathbf{x}_0)$
- Initial velocity $\quad \hat{v}_i(\mathbf{x}_0, 0) = \hat{v}_{0i}(\mathbf{x}_0)$
- Initial stress $\quad \hat{\sigma}_{ij}(\mathbf{x}_0, 0) = \hat{\sigma}_{0ij}(\mathbf{x}_0)$

Owing to the spatial dependency we also need boundary conditions. Since the system contains two first order space derivatives, the spatial dependency of the system is of order two. Therefore, exactly one condition at each boundary point is needed for the problem to have a unique solution.

In this thesis we consider the following two types of boundary conditions:

- Displacement (or Dirichlet) boundary conditions $\hat{u}_i(\mathbf{x}_0, t) = \hat{U}_i(t)$ for $\mathbf{x}_0 \in \partial\Omega_u$
- Traction (or Neumann) boundary conditions $\hat{\sigma}_{ij}(\mathbf{x}_0, t)\hat{n}_j = \hat{\tau}_i(t)$ for $\mathbf{x}_0 \in \partial\Omega_\tau$

where $\hat{\mathbf{n}}$ is the unit vector normal to the prescribed traction boundary $\partial\Omega_\tau$ and pointing outward. It should be noted that the velocity profile at the prescribed displacement boudary $\partial\Omega_u$ is automatically determined by the displacement boundary conditions.

Since each boundary point needs exactly one boundary condition, we find that the prescribed displacement boundary $\partial\Omega_u$ and the prescribed traction boundary $\partial\Omega_\tau$ do not overlap and together form the complete boundary, see Figure 1.3.

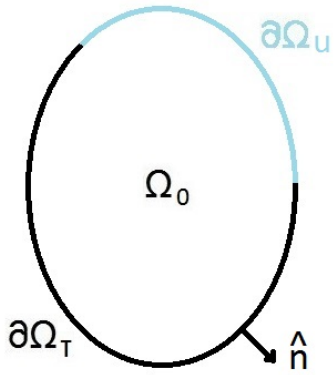

Figure 1.3: Prescribed displacement boundary $\partial\Omega_u$ and prescribed traction boundary $\partial\Omega_\tau$

1.3. ONE DIMENSIONAL PROBLEM

Consider a soil sample of height H that is deformed through loading p_0 on the top with the bottom being fixed. Lateral deformation is prohibited along its sides, so that this problem becomes one dimensional. The case illustrated in Figure 1.4 refers to an oedometer test, a laboratory test used to determine stiffness parameters of soil samples.

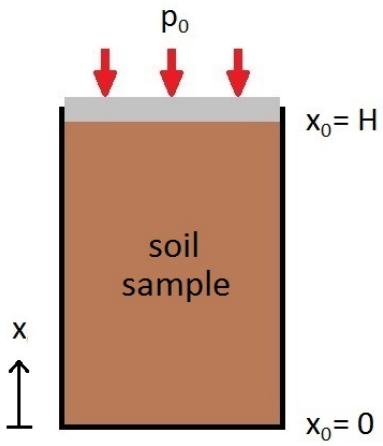

Figure 1.4: Schematic overview of an oedometer test

When a soil sample is considered to be a 1-phase continuum, the 1-phase formulation can be applied. Since the deformation is one dimensional, Equation 1.13 reduces to

$$\begin{aligned} \rho \frac{\partial \hat{v}}{\partial t} &= \frac{\partial \hat{\sigma}}{\partial x_0} - \rho g, \\ \frac{\partial \hat{\sigma}}{\partial t} &= E \frac{\partial \hat{v}}{\partial x_0}, \\ \frac{\partial \hat{u}}{\partial t} &= \hat{v}. \end{aligned} \tag{1.14}$$

Note that in Equation 1.14 the subscripts are omitted. The coordinate x now refers to the vertical direction.

For the special case of oedometer deformation we find a displacement boundary condition at the bottom

$$\hat{u}(0,t) = 0 \tag{1.15}$$

and a traction boundary condition at the top

$$\hat{\sigma}(H,t) = p_0 \tag{1.16}$$

where p_0 is the load applied on the top surface and $p_0 < 0$ corresponds to a load pointing downward.

When we consider the initial state of the sample as the reference state, we find

$$\hat{u}(x_0,0) = 0, \tag{1.17}$$

Since the sample is initially at rest, we also have

$$\hat{v}(x_0,0) = 0, \tag{1.18}$$

Finally, we assume

$$\hat{\sigma}(x_0,0) = 0. \tag{1.19}$$

Note that the system of partial differential equations with these initial and boundary conditions is equivalent to the non-homogeneous wave equation

$$\frac{\partial^2 \hat{u}}{\partial t^2} = \frac{E}{\rho} \frac{\partial^2 \hat{u}}{\partial x_0^2} - g, \qquad 0 < x_0 < H,\ t > 0, \tag{1.20}$$

with initial conditions and boundary conditions

$$\hat{u}(x_0,0) = 0, \qquad \frac{\partial \hat{u}}{\partial t}(x_0,0) = 0, \qquad \hat{u}(0,t) = 0, \qquad E \frac{\partial \hat{u}}{\partial x_0}(H,t) = p_0. \tag{1.21}$$

This system has an analytical solution

$$\hat{u}(x_0,t) = \frac{1}{2}\frac{\rho g}{E} x_0^2 + \frac{p_0 - \rho g H}{E} x_0 + \sum_{n=1}^{\infty} \hat{u}_n \cos\sqrt{\frac{E}{\rho}} \frac{(2n-1)\pi t}{2H} \sin \frac{(2n-1)\pi x_0}{2H}, \tag{1.22}$$

with coefficients

$$\hat{u}_n = \frac{8\left(2\pi p_0 n(-1)^n + 2\rho g H - \pi p_0 (-1)^n\right) H}{\left(4n^2 - 4n + 1\right)(2n-1)\pi^3 E}. \tag{1.23}$$

The derivation of this solution can be found in Appendix A.

In Figure 1.5 the oedometric deformation $x(x_0, t)$ of a 1-phase continuum is plotted for 4 different values of x_0 considering the given exemplary parameters. Only the first four terms of the infinite sum are used, since the coefficients $\hat{u}_n$ are less than 1% of the first coefficient $\hat{u}_1$ for $n \geq 5$.

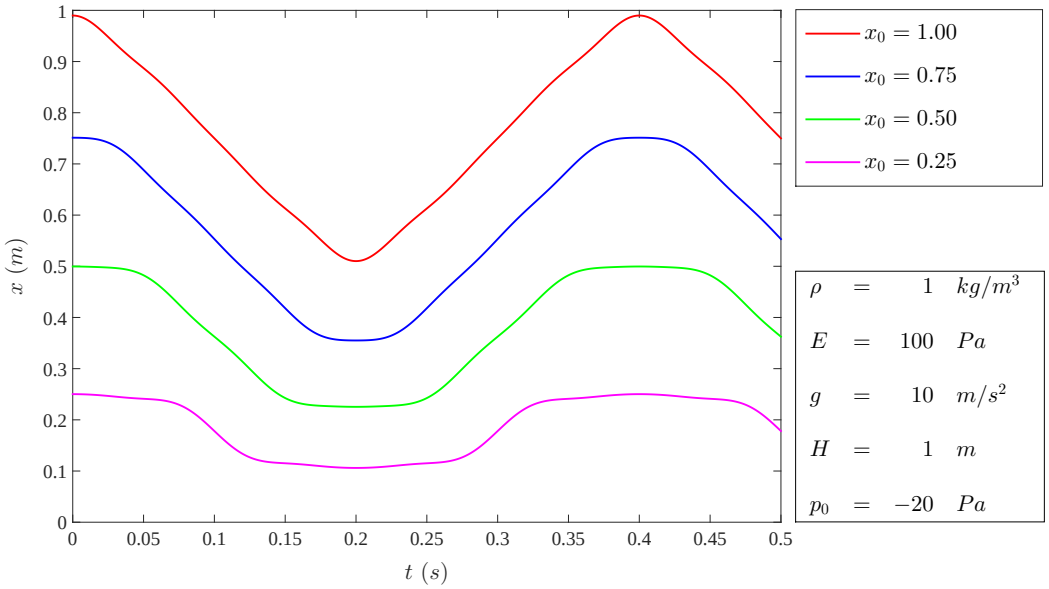

Figure 1.5: Analytical solution for the one dimensional oedometer problem with exemplary parameters

2

FINITE ELEMENT SPACE DISCRETIZATION

This chapter introduces the finite element method (FEM) for the solution of the one dimensional deformation problem of Section 1.3, repeated here

$$\begin{aligned} \rho \frac{\partial \hat{v}}{\partial t} &= \frac{\partial \hat{\sigma}}{\partial x_0} - \rho g, \\ \frac{\partial \hat{\sigma}}{\partial t} &= E \frac{\partial \hat{v}}{\partial x_0}, \\ \frac{\partial \hat{u}}{\partial t} &= \hat{v}. \end{aligned} \tag{2.1}$$

with initial conditions

$$\hat{v}(x_0,0) = 0, \quad \hat{\sigma}(x_0,0) = 0, \quad \hat{u}(x_0,0) = 0, \tag{2.2}$$

and boundary conditions

$$\hat{v}(0,t) = 0, \quad \hat{\sigma}(H,t) = p_0. \tag{2.3}$$

With FEM a spatial domain is divided into a finite number of elements. The method is a result of the combination of matrix structural analysis, variational approximation theory and the introduction of digital computers. Turner first introduced FEM to structural problems in aerospace engineering in the early 1950s, while Zienkiewicz introduced the method to non-structural problems such as heat conduction in the mid 1960s [11].

In this study the engineering-oriented approach to FEM is followed, which focuses on its practical application and the analogy to the virtual work equation [12]. In Section 2.1 the momentum equation is transformed into the virtual work equation. In order to discretize the virtual work equation 2-noded line elements with linear interpolation functions are introduced in Section 2.2, which are the one dimensional equivalent of 4-noded tetrahedral elements used later when considering stability of the 2-phase formulation in three dimensions. Then the global matrices belonging to the virtual work equation are expressed in Section 2.3 by assembling them from element matrices. Finally the resulting system of ordinary differential equations is presented in Section 2.4.

2.1. VIRTUAL WORK EQUATION

The virtual work equation is the weak form of the momentum equation, which in one dimension equals

$$\rho \frac{\partial \hat{v}}{\partial t} = \frac{\partial \hat{\sigma}}{\partial x_0} - \rho g. \tag{2.4}$$

The virtual work equation is obtained by multiplying the momentum equation by a virtual velocity $\delta\hat{v}$ and integrating over the domain $0 < x < H$

$$\int_0^H \delta\hat{v}\rho \frac{\partial \hat{v}}{\partial t} dx_0 = \int_0^H \delta\hat{v} \frac{\partial \hat{\sigma}}{\partial x_0} dx_0 - \int_0^H \delta\hat{v}\rho g dx_0. \tag{2.5}$$

The virtual velocity $\delta\hat{v}$ may take arbitrary values complying with applied boundary conditions.

Next, integration by parts is applied to the first term on the right hand side of Equation 2.5, and after applying the boundary conditions for the stress, $\sigma(H,t) = p_0$, and the virtual velocity, $\delta\hat{v}(0,t) = 0$, the virtual work equation becomes

$$\int_0^H \delta\hat{v}\rho\frac{\partial\hat{v}}{\partial t}dx_0 \quad = \quad -\int_0^H \frac{\partial(\delta\hat{v})}{\partial x_0}\hat{\sigma}dx_0 + \delta\hat{v}(H,t)p_0 - \int_0^H \delta\hat{v}\rho g dx_0. \tag{2.6}$$

2.2. LINE ELEMENTS WITH LINEAR INTERPOLATION FUNCTIONS

The initial domain Ω_0 is divided into a finite number of 2-noded line elements Ω_e as illustrated in Figure 2.1. All elements are numbered from 1 to n_e, as well as all nodes from 1 to n_n. When we consider a uniform grid, as in the following, all elements have the same initial length $\Delta x_0 = H/n_e$.

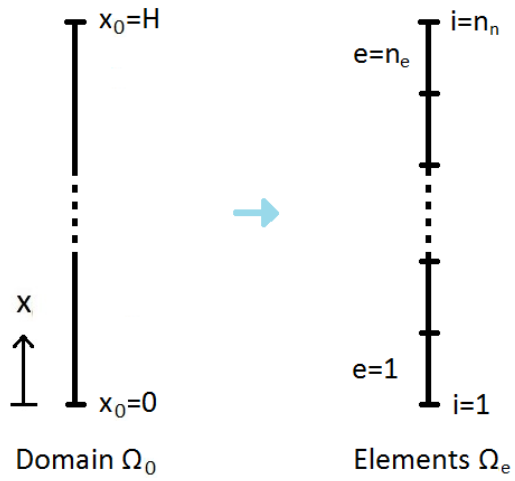

Figure 2.1: Space discretization of domain Ω_0 with finite elements Ω_e

In this particular problem it is easy to see that we have $n_n = n_e + 1$. However, this equality does not hold in general. Consider e.g. a 3-noded line element in one dimension, or a 4-noded tetrahedral element in three dimensions.

Based on this space discretization the displacement, velocity and virtual velocity fields are approximated with linear interpolation functions, also commonly called shape functions

$$\begin{aligned} \hat{u}(x_0,t) &\approx \mathbf{N}(x_0)\mathbf{u}(t), \\ \hat{v}(x_0,t) &\approx \mathbf{N}(x_0)\mathbf{v}(t), \\ \delta\hat{v}(x_0,t) &\approx \mathbf{N}(x_0)\delta\mathbf{v}(t). \end{aligned} \tag{2.7}$$

where vectors $\mathbf{u}(t)$, $\mathbf{v}(t)$ and $\delta\mathbf{v}(t)$ are nodal values

$$\begin{aligned} \mathbf{u}(t) &= \begin{bmatrix} u_1(t) & u_2(t) & \cdots & u_{n_n}(t) \end{bmatrix}^T, \\ \mathbf{v}(t) &= \begin{bmatrix} v_1(t) & v_2(t) & \cdots & v_{n_n}(t) \end{bmatrix}^T, \\ \delta\mathbf{v}(t) &= \begin{bmatrix} \delta v_1(t) & \delta v_2(t) & \cdots & \delta v_{n_n}(t) \end{bmatrix}^T. \end{aligned} \tag{2.8}$$

The interpolation function vector $\mathbf{N}(x_0)$ is

$$\mathbf{N}(x_0) \quad = \quad \begin{bmatrix} N_1(x_0) & N_2(x_0) & \cdots & N_{n_n(x_0)} \end{bmatrix}, \tag{2.9}$$

with linear interpolation functions $N_i(x_j) = \delta_{ij}$ (see Figure 2.2).

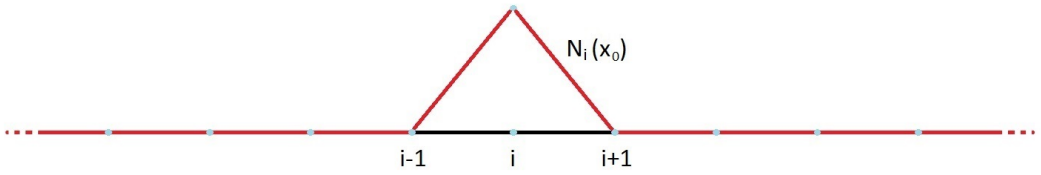

Figure 2.2: Linear interpolation function $N_i(x)$ of node i

The stress field has to be discretized too. We use a different interpolation function vector $\mathbf{K}(x_0)$ for this purpose

$$\hat{\sigma}(x_0,t) \approx \mathbf{K}(x_0)\boldsymbol{\sigma}(t). \tag{2.10}$$

Throughout this thesis step functions $K_e(x_0)$ are chosen such that $K_e(x_0 \in \Omega_f) = \delta_{ef}$, which means that the stress field is assumed to be constant within each element, see Figure 2.3.

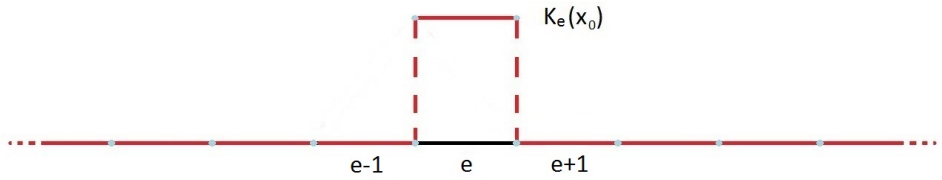

Figure 2.3: Step function $K_e(x)$ for element e

The interpolation function vector $\mathbf{K}(x_0)$ then becomes

$$\mathbf{K}(x_0) = \begin{bmatrix} K_1(x_0) & K_2(x_0) & \cdots & K_{n_e}(x_0) \end{bmatrix}, \tag{2.11}$$

and the vector $\boldsymbol{\sigma}(t)$ is ordered per element

$$\boldsymbol{\sigma}(t) = \begin{bmatrix} \sigma_1(t) & \sigma_2(t) & \cdots & \sigma_{n_e}(t) \end{bmatrix}^T. \tag{2.12}$$

2.3. GLOBAL AND ELEMENT MATRICES OF THE VIRTUAL WORK EQUATION

When all terms of the virtual work equation are replaced by their discretized variants, it becomes

$$\int_0^H (\mathbf{N}\delta\mathbf{v})^T \rho \mathbf{N} \frac{d\mathbf{v}}{dt} dx_0 = -\int_0^H \left(\frac{d\mathbf{N}}{dx_0}\delta\mathbf{v}\right)^T \mathbf{K}\boldsymbol{\sigma}\, dx_0 + (\mathbf{N}(H)\delta\mathbf{v})^T p_0 - \int_0^H (\mathbf{N}\delta\mathbf{v})^T \rho g\, dx_0. \tag{2.13}$$

The expression simplifies when brackets are expanded

$$\delta\mathbf{v}^T \int_0^H \mathbf{N}^T \rho \mathbf{N} dx_0 \frac{d\mathbf{v}}{dt} = -\delta\mathbf{v}^T \int_0^H \left(\frac{d\mathbf{N}}{dx_0}\right)^T \mathbf{K} dx_0 \boldsymbol{\sigma} + \delta\mathbf{v}^T \mathbf{N}(H)^T p_0 - \delta\mathbf{v}^T \int_0^H \mathbf{N}^T \rho g\, dx_0. \tag{2.14}$$

Since the virtual velocity is arbitrarily chosen, Equation 2.14 may be written as

$$\int_0^H \mathbf{N}^T \rho \mathbf{N} dx_0 \frac{d\mathbf{v}}{dt} = -\int_0^H \left(\frac{d\mathbf{N}}{dx_0}\right)^T \mathbf{K} dx_0 \boldsymbol{\sigma} + \mathbf{N}(H)^T p_0 - \int_0^H \mathbf{N}^T \rho g\, dx_0, \tag{2.15}$$

which yields in matrix notation

$$\mathbf{M}\frac{d\mathbf{v}}{dt} = -\mathbf{K}^\sigma \boldsymbol{\sigma} + \mathbf{F}^{trac} + \mathbf{F}^{grav}. \tag{2.16}$$

The matrix $\mathbf{M}$ is called the global mass matrix. On the right hand side, vector $\mathbf{K}^{\sigma}\boldsymbol{\sigma}$ represents the internal forces and global external force vectors $\mathbf{F}^{trac}$ and $\mathbf{F}^{grav}$ are assembled from the traction forces and the gravitational forces respectively.

The global matrices are assembled from element matrices of elements $1,\ldots,n_e$. These element matrices are constructed by elementwise integration of the virtual work equation over elements e with nodes i and $i+1$

$$\int_{x_i}^{x_{i+1}} \mathbf{N}_e^T \rho \mathbf{N}_e dx_0 \frac{d\mathbf{v}_e}{dt} = -\int_{x_i}^{x_{i+1}} \left(\frac{d\mathbf{N}_e}{dx_0}\right)^T \mathbf{K}_e dx_0 \boldsymbol{\sigma}_e + \mathbf{N}_e(H)^T p_0 - \int_{x_i}^{x_{i+1}} \mathbf{N}_e^T \rho g dx_0, \tag{2.17}$$

where $\mathbf{N}_e = \begin{bmatrix} N_i & N_{i+1} \end{bmatrix}$, $\mathbf{v}_e = \begin{bmatrix} v_i & v_{i+1} \end{bmatrix}^T$, $\mathbf{K}_e = \begin{bmatrix} K_e \end{bmatrix}$ and $\boldsymbol{\sigma}_e = \begin{bmatrix} \sigma_e \end{bmatrix}^T$ since by definition only nodes i and $i+1$ matter in element e.

In matrix notation Equation 2.17 becomes

$$\mathbf{M}_e \frac{d\mathbf{v}_e}{dt} = -\mathbf{K}_e^{\sigma}\boldsymbol{\sigma}_e + \mathbf{F}_e^{trac} + \mathbf{F}_e^{grav}. \tag{2.18}$$

The matrix $\mathbf{M}_e$ is called the element mass matrix and the vectors $\mathbf{K}_e^{\sigma}\boldsymbol{\sigma}_e$, $\mathbf{F}_e^{trac}$ and $\mathbf{F}_e^{grav}$ store the corresponding nodal forces of element e.

In order to be able to solve the ordinary differential equations, the integrals of Equation 2.17 need to be computed. Therefore we firstly transform the integrals from the global coordinate to a local coordinate, given by

$$x_0 = x_i + (x_{i+1} - x_i)\,\xi = x_i + \Delta x_0\,\xi \tag{2.19}$$

with ξ being the local coordinate (see Figure 2.4).

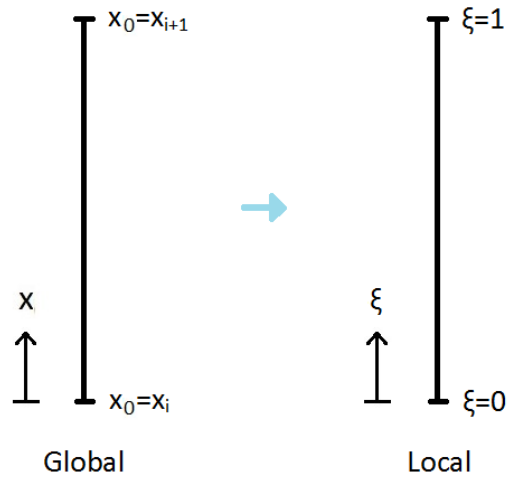

Figure 2.4: Global and local coordinate within element e

For the local coordinate the considered linear interpolation functions $\mathbf{N}_e$ become

$$\mathbf{N}_e = \begin{bmatrix} 1-\xi & \xi \end{bmatrix} \tag{2.20}$$

The result of the transformation is

$$\int_0^1 \mathbf{N}_e^T \rho \mathbf{N}_e \Delta x_0 d\xi \frac{d\mathbf{v}_e}{dt} = -\int_0^1 \left(\frac{d\mathbf{N}_e}{d\xi}\right)^T \mathbf{K}_e d\xi \boldsymbol{\sigma}_e + \mathbf{N}_e(H)^T p_0 - \int_0^1 \mathbf{N}_e^T \rho g \Delta x_0 d\xi. \tag{2.21}$$

Since in most cases it is not possible to apply closed form integration, it is necessary to approximate the integrals numerically. In this thesis, Gaussian quadrature with a single Gauss point is used, see Appendix C.1, corresponding to the Deltares MPM code. It should be noted that this reduced integration method is equal to the midpoint rule in one dimension.

The application of Gaussian quadrature to Equation 2.21 results in

$$\begin{bmatrix} \frac{1}{4}\rho\Delta x_0 & \frac{1}{4}\rho\Delta x_0 \\ \frac{1}{4}\rho\Delta x_0 & \frac{1}{4}\rho\Delta x_0 \end{bmatrix} \frac{d\mathbf{v}_e}{dt} = -\begin{bmatrix} -1 \\ 1 \end{bmatrix} \boldsymbol{\sigma}_e + \mathbf{N}_e(H)^T p_0 + \begin{bmatrix} -\frac{1}{2}\rho g\Delta x_0 \\ -\frac{1}{2}\rho g\Delta x_0 \end{bmatrix}. \tag{2.22}$$

We are now able to assemble the global matrices from the element matrices by using the assemblage procedure from Appendix C.2, which renders

$$\mathbf{M} = \begin{bmatrix} \frac{1}{4}\rho\Delta x_0 & \frac{1}{4}\rho\Delta x_0 & & & 0 \\ \frac{1}{4}\rho\Delta x_0 & \frac{1}{2}\rho\Delta x_0 & \ddots & & \\ & \ddots & \ddots & \ddots & \\ & & \ddots & \frac{1}{2}\rho\Delta x_0 & \frac{1}{4}\rho\Delta x_0 \\ 0 & & & \frac{1}{4}\rho\Delta x_0 & \frac{1}{4}\rho\Delta x_0 \end{bmatrix} \quad \mathbf{K}^{\sigma} = \begin{bmatrix} -1 & & & & 0 \\ 1 & -1 & & & \\ & \ddots & \ddots & & \\ & & 1 & -1 & \\ 0 & & & & 1 \end{bmatrix} \tag{2.23}$$

When the same procedure is applied to the external force vectors, we find

$$\mathbf{F}^{trac} = \begin{bmatrix} 0 \\ 0 \\ \vdots \\ 0 \\ p_0 \end{bmatrix} \quad \mathbf{F}^{grav} = \begin{bmatrix} -\frac{1}{2}\rho g\Delta x_0 \\ -\rho g\Delta x_0 \\ \vdots \\ -\rho g\Delta x_0 \\ -\frac{1}{2}\rho g\Delta x_0 \end{bmatrix} \tag{2.24}$$

Of course the assemblage procedure can be performed easily on a computer.

In order to solve the ordinary differential Equation 2.16 it is necessary to compute the inverse of the mass matrix $\mathbf{M}$. Inverting it repeatedly requires considerable computation time in case of large systems of equations as encountered with geomechanical problems. Alternatively, we can use the lumped mass matrix $\mathbf{M}^L$ which is a diagonal matrix. Appendix C.3 explains how the lumped mass matrix is constructed from the mass matrix using the lumping procedure.

$$\mathbf{M}^L = \begin{bmatrix} \frac{1}{2}\rho\Delta x_0 & & & & 0 \\ & \rho\Delta x_0 & & & \\ & & \ddots & & \\ & & & \rho\Delta x_0 & \\ 0 & & & & \frac{1}{2}\rho\Delta x_0 \end{bmatrix} \tag{2.25}$$

Using the lumped mass matrix renders slightly less accurate results, but saves computation time and storage space.

2.4. RESULTING SYSTEM OF ORDINARY DIFFERENTIAL EQUATIONS

To conclude this Chapter we summarize the system of the ordinary differential equations

$$\begin{aligned} \mathbf{M}^L \frac{d\mathbf{v}}{dt} &= -\mathbf{K}^\sigma \boldsymbol{\sigma} + \mathbf{F}^{trac} + \mathbf{F}^{grav}, \\ \frac{d\boldsymbol{\sigma}}{dt} &= \mathbf{K}^v \mathbf{v}, \\ \frac{d\mathbf{u}}{dt} &= \mathbf{v}, \end{aligned} \tag{2.26}$$

with initial conditions

$$\mathbf{v}(0) = \mathbf{0}, \quad \boldsymbol{\sigma}(0) = \mathbf{0}, \quad \mathbf{u}(0) = \mathbf{0}. \tag{2.27}$$

The global matrix $\mathbf{K}^v$ and element matrices $\mathbf{K}^v_e$ follow from the rather trivial discretization of the considered constitutive relation

$$\mathbf{K}^v = \begin{bmatrix} -\frac{E}{\Delta x_0} & \frac{E}{\Delta x_0} & & & 0 \\ & \ddots & \ddots & & \\ & & & \ddots & \ddots \\ 0 & & & -\frac{E}{\Delta x_0} & \frac{E}{\Delta x_0} \end{bmatrix}, \qquad \mathbf{K}^v_e = \begin{bmatrix} -\frac{E}{\Delta x_0} & \frac{E}{\Delta x_0} \end{bmatrix}. \tag{2.28}$$

The matrix $\mathbf{K} = \mathbf{K}^\sigma \mathbf{K}^v$ is referred to as the stiffness matrix.

3

EULER-CROMER TIME DISCRETIZATION

For the time discretization of the system of ordinary differential Equations 2.26 we use the Euler-Cromer method [13]. Preference was given to this scheme above other one-step schemes as it is energy conserving, conditionally stable, first order accurate and most important it avoids iteration procedures within a time step [3].

The Euler-Cromer method can be applied to Hamiltonian equations, differential equations of the form

$$\begin{aligned} \frac{dx}{dt} &= f(y,t), \\ \frac{dy}{dt} &= g(x,t). \end{aligned} \tag{3.1}$$

The explicit Euler method is applied to the first equation and the implicit Euler method to the second

$$\begin{aligned} x^{n+1} &= x^n + \Delta t f(y^n, t^n), \\ y^{n+1} &= y^n + \Delta t g(x^{n+1}, t^n). \end{aligned} \tag{3.2}$$

where Δt denotes the chosen interval of a time step.
Recall the system of ordinary differential equations from Section 2.4

$$\begin{aligned} \mathbf{M}^L \frac{d\mathbf{v}}{dt} &= -\mathbf{K}^\sigma \boldsymbol{\sigma} + \mathbf{F}^{trac} + \mathbf{F}^{grav}, \\ \frac{d\boldsymbol{\sigma}}{dt} &= \mathbf{K}^v \mathbf{v}, \\ \frac{d\mathbf{u}}{dt} &= \mathbf{v}, \end{aligned} \tag{3.3}$$

with initial conditions

$$\mathbf{v}(0) = \mathbf{0}, \quad \boldsymbol{\sigma}(0) = \mathbf{0}, \quad \mathbf{u}(0) = \mathbf{0}. \tag{3.4}$$

Let $\mathbf{v}^n$, $\boldsymbol{\sigma}^n$ and $\mathbf{u}^n$ denote the velocity, stress and displacement respectively at time level $t = n\Delta t$. The initial conditions are now given by

$$\mathbf{v}^0 = \mathbf{0}, \quad \boldsymbol{\sigma}^0 = \mathbf{0}, \quad \mathbf{u}^0 = \mathbf{0}. \tag{3.5}$$

Since the first two equations of Equation 3.3 form a pair of differential equations to which the Euler-Cromer method can be applied, the velocity and stress, on the nodes and Gauss points respectively, can be computed on the next time level with

$$\begin{aligned} \mathbf{v}^{n+1} &= \mathbf{v}^n + \Delta t \left(\mathbf{M}^L\right)^{-1} \left[-\mathbf{K}^\sigma \boldsymbol{\sigma}^n + \mathbf{F}^{trac} + \mathbf{F}^{grav}\right], \\ \boldsymbol{\sigma}^{n+1} &= \boldsymbol{\sigma}^n + \Delta t \mathbf{K}^v \mathbf{v}^{n+1}, \end{aligned} \tag{3.6}$$

assuming constant loads and constant mass and stiffness matrices.

Since the velocity at the next time level is now computed, we add an implicit equation for the displacement

$$\mathbf{u}^{n+1} = \mathbf{u}^n + \Delta t \mathbf{v}^{n+1}. \tag{3.7}$$

For each time step this procedure is repeated as summarized in the flowchart in Figure 3.1.

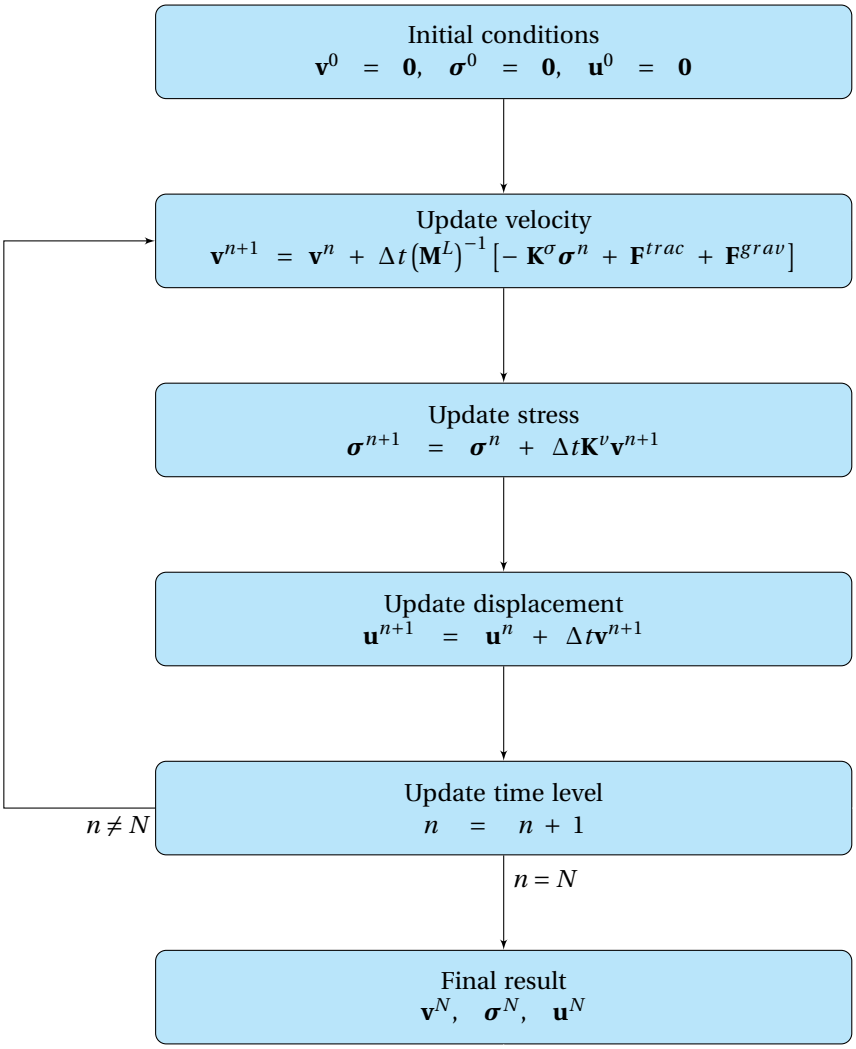

Figure 3.1: Time step procedure for time interval $[0, N\Delta t]$

4

STABILITY ANALYSIS

Numerical methods transform differential equations into discretized equations. However, this does not mean that performing the numerical method on a computer will necessarily lead to the exact solution of the discretized equation. Errors between the computed solution and the exact solution might accumulate for a certain time due to e.g. round-off errors.

A numerical method is called stable if these errors stay bounded, and is otherwise called unstable. However, it is possible that the stability of a numerical method depends on the time step size. Therefore all numerical methods are classified to be unconditionally stable, conditionally stable or unconditionally unstable. Which class a method belongs to can be found with the help of a stability analysis.

In the previous chapters a numerical scheme has been introduced for a one dimensional small deformation problem for 1-phase materials using the finite element method for the space discretization and the Euler-Cromer method for the time discretization. This chapter is devoted to the stability analysis of this numerical scheme considering two different methods for stability analysis. Section 4.1 introduces the Von Neumann method and Section 4.2 the matrix method.

4.1. VON NEUMANN METHOD

At present, one of the most popular methods for stability analysis is the Von Neumann method, sometimes referred to as the Fourier stability analysis, which is extensively described by Hirsch [14].

The starting point of the Von Neumann method is the system of discrete equations derived in Chapter 3

$$\begin{aligned} \mathbf{v}^{n+1} &= \mathbf{v}^n + \Delta t \left(\mathbf{M}^L\right)^{-1} \left[-\mathbf{K}^\sigma \boldsymbol{\sigma}^n + \mathbf{F}^{trac} + \mathbf{F}^{grav} \right], \\ \boldsymbol{\sigma}^{n+1} &= \boldsymbol{\sigma}^n + \Delta t \mathbf{K}^v \mathbf{v}^{n+1}, \\ \mathbf{u}^{n+1} &= \mathbf{u}^n + \Delta t \mathbf{v}^{n+1}. \end{aligned} \tag{4.1}$$

The method assumes periodic boundary conditions, i.e. boundary conditions are not taken into account. Therefore, we are now able to consider only the change of velocity and displacement of internal node i and the change of stress within element i.
The change of velocity of internal node i is retrieved from row i of the corresponding matrix equation

$$v_i^{n+1} = v_i^n + \frac{\Delta t}{\rho \Delta x_0} \left(\sigma_i^n - \sigma_{i-1}^n \right) - \Delta t g. \tag{4.2}$$

We now introduce the displacement operator D defined by $D^k (\cdot)_i^n = (\cdot)_{i+k}^n$ and Equation 4.2 becomes

$$v_i^{n+1} = v_i^n + \frac{\Delta t}{\rho \Delta x_0} \left(1 - D^{-1} \right) \sigma_i^n - \Delta t g. \tag{4.3}$$

In the same way we find

$$\begin{aligned} \sigma_i^{n+1} &= \sigma_i^n + \frac{E\Delta t}{\Delta x_0}(D-1)\, v_i^{n+1}, \\ u_i^{n+1} &= u_i^n + \Delta t\, v_i^{n+1}, \end{aligned} \tag{4.4}$$

Equations 4.3 and 4.4 can be written in operator form as

$$\mathbf{A}(D)\mathbf{x}_i^{n+1} = \mathbf{B}(D)\mathbf{x}_i^n + \mathbf{q} \tag{4.5}$$

where

$$\mathbf{A}(D) = \begin{bmatrix} 1 & 0 & 0 \\ \frac{E\Delta t}{\Delta x_0}(1-D) & 1 & 0 \\ -\Delta t & 0 & 1 \end{bmatrix}, \quad \mathbf{B}(D) = \begin{bmatrix} 1 & \frac{\Delta t}{\rho \Delta x_0}\left(1-D^{-1}\right) & 0 \\ 0 & 1 & 0 \\ 0 & 0 & 1 \end{bmatrix}, \quad \mathbf{q} = \begin{bmatrix} -\Delta t g \\ 0 \\ 0 \end{bmatrix}, \quad \mathbf{x}_i^n = \begin{bmatrix} v_i^n \\ \sigma_i^n \\ u_i^n \end{bmatrix}. \tag{4.6}$$

Assume that the computed solution $\mathbf{x}_i^n$ equals the sum of the exact solution $\hat{\mathbf{x}}_i^n$ and an error $\boldsymbol{\eta}_i^n$. Since $\hat{\mathbf{x}}_i^n$ is the exact solution of Equation 4.5, the error must satisfy the so-called error equation

$$\mathbf{A}(D)\,\boldsymbol{\eta}_i^{n+1} = \mathbf{B}(D)\,\boldsymbol{\eta}_i^n. \tag{4.7}$$

The error can be decomposed into a discrete Fourier series over a finite number of harmonics

$$\boldsymbol{\eta}_i^n = \sum_{j=-N}^{N} \mathbf{a}_j^n e^{Ik_j i\Delta x_0} = \sum_{j=-N}^{N} \mathbf{a}_j^n e^{Ii\phi_j}, \tag{4.8}$$

where I is the unit complex number, a_j^n the amplitude of the jth harmonic at time level n, and k_j the wave number of the jth harmonic. $k_j\Delta x_0$ is often denoted as the phase angle ϕ_j.

Since $\mathbf{A}(D)$ and $\mathbf{B}(D)$ are linear operators, all harmonics should satisfy Equation 4.7. When a single harmonic is inserted into the error equation, the error equation is given by

$$\mathbf{A}(D)\,\mathbf{a}_j^{n+1} e^{Ii\phi_j} = \mathbf{B}(D)\,\mathbf{a}_j^n e^{Ii\phi_j}. \tag{4.9}$$

When the definition of the displacement operator is applied and the subscript j is dropped, we find

$$\mathbf{A}\left(e^{I\phi}\right)\mathbf{a}^{n+1} e^{Ii\phi} = \mathbf{B}\left(e^{I\phi}\right)\mathbf{a}^n e^{Ii\phi}, \tag{4.10}$$

from which we deduce

$$\mathbf{a}^{n+1} = \mathbf{G}(\phi)\mathbf{a}^n \tag{4.11}$$

with amplification matrix $\mathbf{G}(\phi) = \mathbf{A}\left(e^{I\phi}\right)^{-1}\mathbf{B}\left(e^{I\phi}\right)$.

Let $\rho(\mathbf{G}) = \max|\lambda(\mathbf{G})|$ be the spectral radius of the amplification matrix $\mathbf{G}(\phi)$. Richtmyer and Morton [15] show that the Von Neumann necessary criterion for stability is given by

$$\rho(\mathbf{G}) \leq 1 + O(\Delta t) \qquad \forall \phi \in (-\pi, \pi). \tag{4.12}$$

However, for practical reasons it is more convenient to use the strict stability condition by Hirsch [14]

$$\rho(\mathbf{G}) \leq 1 \qquad \forall \phi \in (-\pi, \pi). \tag{4.13}$$

The spectral radius of the amplification matrix is determined by the eigenvalue problem

$$\mathbf{G}(\phi)\mathbf{a} = \lambda \mathbf{a}, \tag{4.14}$$

which is by definition equivalent to the eigenvalue problem

$$\mathbf{B}\left(e^{I\phi}\right)\mathbf{a} = \lambda \mathbf{A}\left(e^{I\phi}\right)\mathbf{a}. \tag{4.15}$$

To compute the eigenvalues λ we solve the characteristic equation

$$\det\left(\mathbf{B}\left(e^{I\phi}\right) - \lambda \mathbf{A}\left(e^{I\phi}\right)\right) = 0. \tag{4.16}$$

Let us first consider the matrix $\mathbf{B}\left(e^{I\phi}\right) - \lambda\mathbf{A}\left(e^{I\phi}\right)$.

$$\mathbf{B}\left(e^{I\phi}\right) - \lambda\mathbf{A}\left(e^{I\phi}\right) \quad = \quad \begin{bmatrix} 1-\lambda & \frac{\Delta t}{\rho\Delta x_0}(1-e^{-I\phi}) & 0 \\ -\lambda\frac{E\Delta t}{\Delta x_0}(1-e^{I\phi}) & 1-\lambda & 0 \\ \lambda\Delta t & 0 & 1-\lambda \end{bmatrix} \tag{4.17}$$

After writing out the determinant, the characteristic equation becomes

$$(1\,-\,\lambda)\left(1\,+\,(4d\,-\,2)\lambda\,+\,\lambda^2\right) \quad = \quad 0, \qquad d\,=\,\frac{E\Delta t^2}{\rho\Delta x_0^2}\sin^2\left(\frac{\phi}{2}\right), \tag{4.18}$$

which has the following roots

$$\lambda_1\,=\,1, \qquad \lambda_{2,3}\,=\,1\,-\,2d\,\pm\,\sqrt{(1\,-\,2d)\,-\,1}. \tag{4.19}$$

The Von Neumann necessary stability criterion of Hirsch results in

$$\left|1\,-\,2d\,\pm\,\sqrt{(1\,-\,2d)^2\,-\,1}\right| \quad \leq \quad 1, \qquad \forall\phi\in(-\pi,\pi). \tag{4.20}$$

This expression can be simplified using the following lemma.

Lemma 4.1. *Let a, b be real numbers that satisfy the inequality*

$$\left|a\,\pm\,\sqrt{a^2\,-\,b}\right| \quad \leq \quad 1. \tag{4.21}$$

Then a, b satisfy

$$-b\,-\,1\,\leq\,2a\,\leq\,b\,+\,1 \qquad \textit{and} \qquad b\,\leq\,1. \tag{4.22}$$

The proof can be found in Appendix D.

Applying Lemma 4.1 to Equation 4.20 renders

$$-2\,\leq\,2\,-\,4d\,=\,2\,-\,4\frac{E\Delta t^2}{\rho\Delta x_0^2}\sin^2\left(\frac{\phi}{2}\right)\,\leq\,2, \qquad \forall\phi\in(-\pi,\pi), \tag{4.23}$$

which is satisfied when

$$0\,\leq\,\frac{E\Delta t^2}{\rho\Delta x_0^2}\,\leq\,1. \tag{4.24}$$

That is, the numerical method is stable when the applied time step size satisfies

$$0\,\leq\,\Delta t\,\leq\,\frac{\Delta x_0}{\sqrt{E/\rho}} \tag{4.25}$$

and unstable otherwise.

4.2. MATRIX METHOD

The matrix method uses another approach. It starts with the ordinary differential equations of Section 2.4, repeated here

$$\begin{aligned} \mathbf{M}^L\frac{d\mathbf{v}}{dt} &= -\mathbf{K}^\sigma\boldsymbol{\sigma}\,+\,\mathbf{F}^{trac}\,+\,\mathbf{F}^{grav}, \\ \frac{d\boldsymbol{\sigma}}{dt} &= \mathbf{K}^v\mathbf{v}, \\ \frac{d\mathbf{u}}{dt} &= \mathbf{v}, \end{aligned} \tag{4.26}$$

Owing to the semi-implicit character of the Euler-Cromer method, it is necessary to transform the system of first order ordinary differential equations into the second order ordinary differential equation

$$\mathbf{M}^L \frac{d^2\mathbf{u}}{dt^2} = -\mathbf{K}^\sigma \mathbf{K}^\nu \mathbf{u} + \mathbf{F}^{trac} + \mathbf{F}^{grav}, \tag{4.27}$$

with corresponding error equation

$$\mathbf{M}^L \frac{d^2\boldsymbol{\eta}}{dt^2} = -\mathbf{K}^\sigma \mathbf{K}^\nu \boldsymbol{\eta} \tag{4.28}$$

Now the problem is uncoupled by solving the eigenvalue problem

$$\mathbf{K}^\sigma \mathbf{K}^\nu \mathbf{v} = \lambda \mathbf{M}^L \mathbf{v}. \tag{4.29}$$

This is a large eigenvalue problem when considering a larger mesh, but according to Irons [16] we may estimate the eigenvalues by the eigenvalues of the corresponding element matrices

$$\lambda_e^{min} \leq \lambda \leq \lambda_e^{max} \tag{4.30}$$

which follow from the smaller eigenvalue problem

$$\mathbf{K}_e^\sigma \mathbf{K}_e^\nu \mathbf{v} = \lambda_e \mathbf{M}_e^L \mathbf{v}. \tag{4.31}$$

Let us first consider the matrix $\mathbf{K}_e^\sigma \mathbf{K}_e^\nu - \lambda_e \mathbf{M}_e^L$

$$\mathbf{K}_e^\sigma \mathbf{K}_e^\nu - \lambda_e \mathbf{M}_e^L = \begin{bmatrix} \frac{E}{\Delta x_0} - \frac{1}{2}\lambda_e \rho \Delta x_0 & -\frac{E}{\Delta x_0} \\ -\frac{E}{\Delta x_0} & \frac{E}{\Delta x_0} - \frac{1}{2}\lambda_e \rho \Delta x_0 \end{bmatrix} \tag{4.32}$$

which results in the following characteristic equation

$$\frac{1}{4}\lambda_e \rho \left(\lambda_e \rho \Delta x_0^2 - 4E\right) = 0. \tag{4.33}$$

The roots of the characteristic equation equal

$$\lambda_{e,1} = 0, \qquad \lambda_{e,2} = \frac{4E}{\rho \Delta x_0^2}. \tag{4.34}$$

For the eigenvalues of the large eigenvalue problem we thus know

$$0 \leq \lambda \leq \frac{4E}{\rho \Delta x_0^2}. \tag{4.35}$$

We are now able to reconsider the ordinary differential Equation 4.28 as

$$\frac{d^2\boldsymbol{\eta}}{dt^2} = -\lambda \boldsymbol{\eta} \tag{4.36}$$

or componentwise

$$\frac{d^2\eta_j}{dt^2} = -\lambda \eta_j, \tag{4.37}$$

when $\boldsymbol{\eta}$ is the eigenvector corresponding to eigenvalue λ.

The next step is to transform the second order differential Equation 4.37 back into a system of first order differential equations

$$\begin{cases} \frac{d\eta_{j1}}{dt} = -\lambda \eta_{j2}, \\ \frac{d\eta_{j2}}{dt} = \eta_{j1} \end{cases} \tag{4.38}$$

and apply Euler-Cromer method to it

$$\eta_{j1}^{n+1} = \eta_{j1}^{n} - \Delta t \lambda \eta_{2j}^{n}, \tag{4.39}$$

$$\eta_{j2}^{n+1} = \eta_{j2}^{n} + \Delta t \eta_{j1}^{n+1}. \tag{4.40}$$

In matrix notation this becomes

$$\begin{bmatrix} 1 & 0 \\ -\Delta t & 1 \end{bmatrix} \begin{bmatrix} \eta_{j1}^{n+1} \\ \eta_{j2}^{n+1} \end{bmatrix} = \begin{bmatrix} 1 & -\lambda\Delta t \\ 0 & 1 \end{bmatrix} \begin{bmatrix} \eta_{j1}^{n} \\ \eta_{j2}^{n} \end{bmatrix}. \tag{4.41}$$

We get the eigenvalues μ from the corresponding eigenvalue problem

$$\mu_{1,2} = 1 - \frac{1}{2}\lambda\Delta t^2 \pm \sqrt{\left(1 - \frac{1}{2}\lambda\Delta t^2\right)^2 - 1} \tag{4.42}$$

In order for the method to be stable $|\mu| \leq 1$ must hold and according to Lemma 4.1 this equals

$$-2 \leq 2 - \lambda\Delta t^2 \leq 2 \tag{4.43}$$

which is satisfied when

$$0 \leq \lambda\Delta t^2 \leq 4. \tag{4.44}$$

Taking into account the estimate for λ in Equation 4.35,we find

$$0 \leq \frac{E\Delta t^2}{\rho\Delta x_0^2} \leq 1, \tag{4.45}$$

or equivalently

$$0 \leq \Delta t \leq \frac{\Delta x_0}{\sqrt{E/\rho}}. \tag{4.46}$$

As expected, the matrix method gives the same stability criterion as the Von Neumann method.

5

VALIDATION OF OBTAINED STABILITY CRITERION

After performing the finite element space discretization in Chapter 2 and the Euler-Cromer time discretization in Chapter 3 the one dimensional oedometric deformation of a 1-phase continuum presented in Section 1.3 equals

$$\begin{aligned} \mathbf{v}^{n+1} &= \mathbf{v}^n + \Delta t \left(\mathbf{M}^L\right)^{-1} \left[-\mathbf{K}^\sigma \boldsymbol{\sigma}^n + \mathbf{F}^{trac} + \mathbf{F}^{grav} \right], \\ \boldsymbol{\sigma}^{n+1} &= \boldsymbol{\sigma}^n + \Delta t \mathbf{K}^v \mathbf{v}^{n+1}, \\ \mathbf{u}^{n+1} &= \mathbf{u}^n + \Delta t \mathbf{v}^{n+1}, \end{aligned} \tag{5.1}$$

with initial conditions

$$\mathbf{v}^0 = \mathbf{0}, \quad \boldsymbol{\sigma}^0 = \mathbf{0}, \quad \mathbf{u}^0 = \mathbf{0}. \tag{5.2}$$

The numerical solution has been computed using Matlab. Since the analytical solution of the differential equation is available it is possible to validate the stability criterion that followed from the Von Neumann method in Section 4.1 and the matrix method in Section 4.2

$$0 \leq \Delta t \leq \frac{\Delta x_0}{\sqrt{E/\rho}}. \tag{5.3}$$

The exemplary parameters in Table 5.1 give us the following critical time step

$$\Delta t_{crit} = \frac{\Delta x_0}{\sqrt{E/\rho}} = 0.001\ s. \tag{5.4}$$

ρ	=	2	kg/m^3	g	=	10	m/s^2
E	=	100	Pa	p_0	=	-20	Pa
H	=	1	m	Δx_0	=	0.01	m

Table 5.1: List of exemplary parameters

In Figure 5.1 the numerical solution is compared to the analytical solution for 4 different values of x_0. For the considered parameters and a time step of $\Delta t = 0.99\Delta t_{crit}$ the numerical method is indeed stable.

However, when considering a time step $\Delta t = 1.01\Delta t_{crit}$ that does not satisfy the stability criterion, the numerical method is indeed unstable. Figure 5.2 shows that the numerical solution quickly deviates from the analytical solution.

The correctness of the stability criterion was already expected since the criterion is consistent with the well-known CFL (Courant, Friedrichs and Lewy) condition [3, 17].

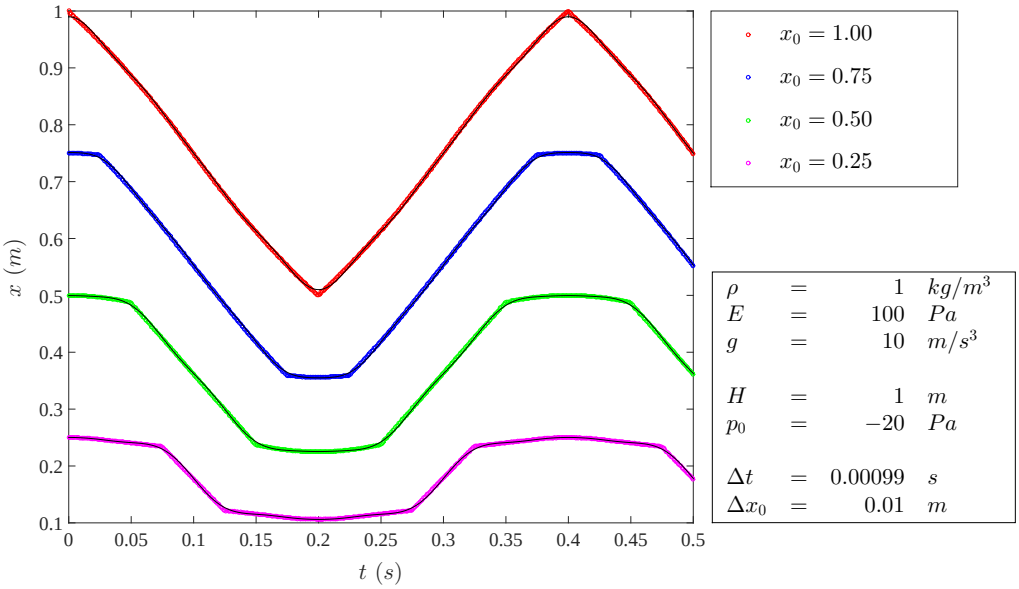

Figure 5.1: Comparison of numerical and analytical solution for 1D oedometer problem for $\Delta t = 0.99\Delta t_{crit}$, rendering stable numerical analysis

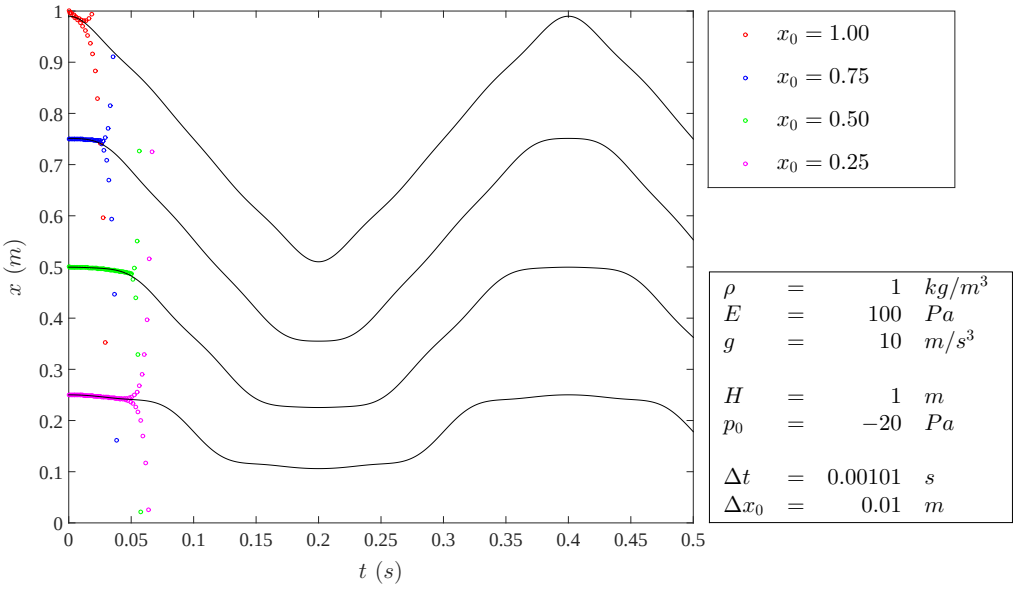

Figure 5.2: Comparison of numerical and analytical solution for 1D oedometer problem for $\Delta t = 1.01\Delta t_{crit}$, rendering unstable numerical analysis

PART II

CONSIDERATION OF SOIL AS A 2-PHASE CONTINUUM

6

PHYSICAL MODEL

This chapter introduces a physical model for small deformations of porous, saturated media, e.g. soil. Such a formulation allows us to simulate the time-delayed settlement due to a gradual dissipation of pore water out of soil upon loading. In Section 6.1 relevant variables and parameters are defined, before presenting the differential equations that describe the deformation of a 2-phase continuum. Section 6.2 then states the necessary number of initial conditions and boundary conditions. In Section 6.3 the one dimensional case is again introduced. The problem is further simplified for the subsequent stability analysis through additional assumptions.

6.1. EQUATIONS

Similar to the 1-phase formulation we consider the initial configuration $\Omega_0 \in \mathbb{R}^3$ and the deformed configuration $\Omega \in \mathbb{R}^3$ in the Cartesian coordinate system. With a 2-phase continuum the deformation of both phases is considered separately.

The displacement and velocity of the solid phase have already been defined in Section 1.1. For the velocity of the liquid phase a new variable is introduced

$$\hat{\mathbf{w}}(\mathbf{x}_0, t) = \begin{bmatrix} \hat{w}_1 & \hat{w}_2 & \hat{w}_3 \end{bmatrix}^T. \tag{6.1}$$

Distinction is made between stresses in the soil skeleton, the effective stresses σ'_{ij}, and the pore water pressure p [18]. They add up to the total stress σ_{ij}

$$\sigma_{ij} = \sigma'_{ij} + p\delta_{ij}, \tag{6.2}$$

where σ and p are defined to be positive in tension and suction respectively. This relation is called the principle of effective stress by Terzaghi [4].

The constitutive relation describes the relation between the stress and strain at the solid phase

$$\frac{\partial \hat{\sigma}'_{ij}}{\partial t} = D_{ijkl} \frac{\partial \hat{\varepsilon}_{kl}}{\partial t} \tag{6.3}$$

with coefficients D_{ijkl} as defined in Equation 1.10 and the strain rate tensor computed from velocity $\mathbf{v}$.

The density and volume of the solid phase are denoted as ρ_s and V_s respectively, the density of the water phase as ρ_w and the volume of the voids as V_v. The porosity n is defined as the ratio of the volume of the voids and the total volume

$$n = \frac{V_v}{V_s + V_v}. \tag{6.4}$$

Since we consider saturated media, the density of the 2-phase continuum equals

$$\rho = n\rho_w + (1-n)\rho_s. \tag{6.5}$$

Using these definitions the conservation of momentum for the solid and liquid phase [3] are given by

$$(1-n)\rho_s \frac{\partial \hat{v}_j}{\partial t} = \frac{\partial \hat{\sigma}'_{ij}}{\partial x_{0i}} + (1-n)\frac{\partial \hat{p}}{\partial x_{0j}} - (1-n)\rho_s g\delta_{j3} + \frac{n^2\rho_w g}{k}(\hat{w}_j - \hat{v}_j) \tag{6.6}$$

$$n\rho_w \frac{\partial \hat{w}_j}{\partial t} = n\frac{\partial \hat{p}}{\partial x_{0j}} - n\rho_w g\delta_{j3} - \frac{n^2\rho_w g}{k}(\hat{w}_j - \hat{v}_j) \tag{6.7}$$

where k denotes the hydraulic conductivity. The last term on the right hand side of the two equations is referred to as 'drag force': the relative movement between solid and liquid phase induces a damping force.

Combining Equations 6.6 and 6.7 yields the conservation of momentum for the 2-phase continuum

$$(1-n)\rho_s \frac{\partial \hat{v}_j}{\partial t} + n\rho_w \frac{\partial \hat{w}_j}{\partial t} = \frac{\partial \hat{\sigma}'_{ij}}{\partial x_{0i}} + \frac{\partial \hat{p}}{\partial x_{0j}} - \rho g\delta_{j3}. \tag{6.8}$$

In order to complete the physical model the conservation of mass is introduced for both phases for both phases [3]

$$\frac{\partial}{\partial t}\left[(1-n)\rho_s\right] + \frac{\partial}{\partial x_j}\left[(1-n)\rho_s \hat{v}_j\right] = 0, \tag{6.9}$$

$$\frac{\partial}{\partial t}\left[n\rho_w\right] + \frac{\partial}{\partial x_j}\left[n\rho_w \hat{w}_j\right] = 0. \tag{6.10}$$

The liquid phase is assumed to be significantly more compressible than the solid phase. Thus it is assumed that the solid phase is incompressible

$$\frac{\partial \rho_s}{\partial t} = 0. \tag{6.11}$$

The liquid phase is assumed to be linearly compressible, expressed by

$$\frac{\partial \rho_w}{\partial \hat{p}} = -\frac{\rho_w}{K_w}, \tag{6.12}$$

where K_w represents the bulk modulus of the liquid phase.

Isolation of the term $\frac{dn}{dt}$ renders in the so-called storage equation

$$\frac{\partial \hat{p}}{\partial t} = \frac{K_w}{n}\left[(1-n)\frac{\partial \hat{v}_j}{\partial x_{0j}} + n\frac{\partial \hat{w}_j}{\partial x_{0j}}\right]. \tag{6.13}$$

In conclusion the deformation of porous, saturated media can be described in a closed coupled system of the velocities $\hat{\mathbf{v}}$ and $\hat{\mathbf{w}}$, the effective stress tensor $\hat{\boldsymbol{\sigma}}'$ and the pore water pressure p. With the considered formulation, the displacement of the solid phase is traced but not the motion of the liquid phase. The relation between the velocity and the displacement of the solid phase is therefore added

$$\begin{aligned}
n\rho_w \frac{\partial \hat{w}_j}{\partial t} &= n\frac{\partial \hat{p}}{\partial x_{0j}} - n\rho_w g\delta_{j3} - \frac{n^2\rho_w g}{k}(\hat{w}_j - \hat{v}_j),\\
(1-n)\rho_s \frac{\partial \hat{v}_j}{\partial t} + n\rho_w \frac{\partial \hat{w}_j}{\partial t} &= \frac{\partial \hat{\sigma}'_{ij}}{\partial x_{0i}} + \frac{\partial \hat{p}}{\partial x_{0j}} - \rho g\delta_{j3},\\
\frac{\partial \hat{p}}{\partial t} &= \frac{K_w}{n}\left[(1-n)\frac{\partial \hat{v}_j}{\partial x_{0j}} + n\frac{\partial \hat{w}_j}{\partial x_{0j}}\right],\\
\frac{\partial \hat{\sigma}'_{ij}}{\partial t} &= D_{ijkl}\frac{d\hat{\varepsilon}_{kl}}{dt},\\
\frac{\partial \hat{u}_j}{\partial t} &= \hat{v}_j.
\end{aligned} \tag{6.14}$$

6.2. INITIAL AND BOUNDARY CONDITIONS

Similar to the 1-phase formulation, the 2-phase formulation is only a well defined problem if the right number of initial and boundary conditions are added, depending on the order of the problem.

Owing to the first order time derivatives in the 2-phase formulation 6.14 we need one initial condition for both velocities, the effective stress, pore pressure and displacement:

- Initial displacement of the solid phase $\hat{u}_i(\mathbf{x}_0, 0) = \hat{u}_{0i}(\mathbf{x}_0)$
- Initial velocity of the solid phase $\hat{v}_i(\mathbf{x}_0, 0) = \hat{v}_{0i}(\mathbf{x}_0)$
- Initial velocity of the liquid phase $\hat{w}_i(\mathbf{x}_0, 0) = \hat{w}_{0i}(\mathbf{x}_0)$
- Initial pore pressure $\hat{p}(\mathbf{x}_0, 0) = \hat{p}_0(\mathbf{x}_0)$
- Initial effective stress $\hat{\sigma}_{ij}(\mathbf{x}_0, 0) = \hat{\sigma}_{0ij}(\mathbf{x}_0)$

Owing to the spatial dependency of order two for each phase, we need exactly one condition for each phase at each boundary point in order to have a well defined problem. Therefore the boundary $\partial\Omega$ is split into a prescribed displacement boundary $\partial\Omega_u$ and a prescribed traction boundary $\partial\Omega_\tau$ for the solid phase (see Figure 6.1a), and into a prescribed displacement boundary $\partial\Omega_w$ and a prescribed pressure boundary $\partial\Omega_p$ for the liquid phase (see Figure 6.1b).

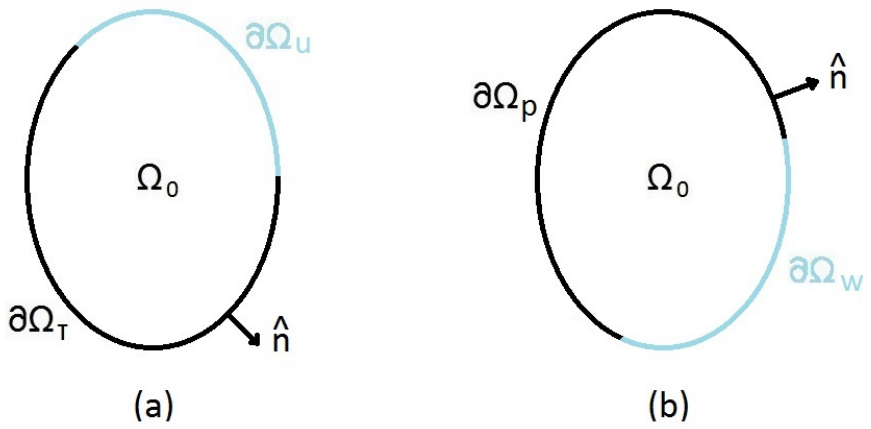

Figure 6.1: (a) Prescribed displacement boundary $\partial\Omega_u$ and prescribed traction boundary $\partial\Omega_\tau$ for the solid phase (b) Prescribed displacement boundary $\partial\Omega_w$ and prescribed pressure boundary $\partial\Omega_p$ for the liquid phase

The two boundary conditions for the solid phase are:

- Displacement (or Dirichlet) boundary conditions $\hat{u}_i(\mathbf{x}_0, t) = \hat{U}_i(t)$ for $\mathbf{x}_0 \in \partial\Omega_u$
- Traction (or Neumann) boundary conditions $\hat{\sigma}'_{ij}(\mathbf{x}_0, t)\hat{n}_j = \hat{\tau}_i(t)$ for $\mathbf{x}_0 \in \partial\Omega_\tau$

The two boundary conditions for the liquid phase are:

- Displacement (or Dirichlet) boundary conditions $\hat{w}_i(\mathbf{x}_0, t) = \hat{W}_i(t)$ for $\mathbf{x}_0 \in \partial\Omega_w$
- Pressure (or Neumann) boundary conditions $\hat{p}(\mathbf{x}_0, t) = \hat{P}(t)$ for $\mathbf{x}_0 \in \partial\Omega_p$

The vector $\hat{\mathbf{n}}$ represents the unit vector normal to the corresponding boundary and pointing outward.

6.3. ONE DIMENSIONAL PROBLEM

In this section we consider the small deformation problem of an oedometer test as described in Section 1.3, but the soil sample is now modeled as a porous, saturated medium. Equations 6.14 thus reduce to

$$\begin{aligned} \rho_w \frac{\partial \hat{w}}{\partial t} &= \frac{\partial \hat{p}}{\partial x_0} - \rho_w g - \frac{n\rho_w g}{k}(\hat{w} - \hat{v}), \\ (1-n)\rho_s \frac{\partial \hat{v}}{\partial t} + n\rho_w \frac{\partial \hat{w}}{\partial t} &= \frac{\partial \hat{\sigma}'}{\partial x_0} + \frac{\partial \hat{p}}{\partial x_0} - \rho g, \\ \frac{\partial \hat{p}}{\partial t} &= \frac{K_w}{n}\left[(1-n)\frac{\partial \hat{v}}{\partial x_0} + n\frac{\partial \hat{w}}{\partial x_0}\right], \\ \frac{\partial \hat{\sigma}'}{\partial t} &= E\frac{\partial \hat{v}}{\partial x_0}, \\ \frac{\partial \hat{u}}{\partial t} &= \hat{v}. \end{aligned} \tag{6.15}$$

The equations are further simplified by adopting some of the assumptions proposed by D. Stolle (personal communication, 2014) in order to simplify the subsequent preliminary stability analysis. Stolle introduces the strong assumption that the liquid phase is incompressible and that the influence of variations in density and porosity in space and time are negligible. Thereby the third equation becomes

$$(1-n)\hat{v} + n\hat{w} = 0, \tag{6.16}$$

and Equations 6.15 reduce to

$$\begin{aligned} \tilde{\rho}\frac{\partial \hat{v}}{\partial t} + \frac{\rho_w g}{k}\hat{v} &= \frac{\partial \hat{\sigma}'}{\partial x_0} - \bar{\rho} g, \\ \frac{d\hat{\sigma}'}{dt} &= E\frac{\partial \hat{v}}{\partial x_0}, \\ \frac{d\hat{u}}{dt} &= \hat{v}. \end{aligned} \tag{6.17}$$

where $\tilde{\rho} = \rho + (\frac{1}{n} - 2)\rho_w$ and $\bar{\rho} = \rho - \rho_w$. Thus, the liquid velocity and pore pressure are no longer relevant variables in the simplified formulation.

As in Section 1.3 a prescribed displacement boundary condition at the bottom and a prescribed traction boundary condition at the top are considered

$$\begin{aligned} \hat{u}(0,t) &= 0, \\ \hat{\sigma}'(H,t) &= p_0. \end{aligned} \tag{6.18}$$

The initial conditions are also inherited from the 1-phase formulation

$$\begin{aligned} \hat{v}(x_0,0) &= 0, \\ \hat{\sigma}'(x_0,0) &= 0, \\ \hat{u}(x_0,0) &= 0. \end{aligned} \tag{6.19}$$

It should be noted that this system of partial differential equations is equivalent to the non-homogeneous damped wave equation

$$\frac{\partial^2 \hat{u}}{\partial t^2} + \frac{\rho_w g}{\tilde{\rho} k}\frac{\partial \hat{u}}{\partial t} = \frac{E}{\tilde{\rho}}\frac{\partial^2 \hat{u}}{\partial x_0^2} - \tilde{g}, \qquad 0 < x_0 < H,\ t > 0 \tag{6.20}$$

with $\tilde{g} = \frac{\bar{\rho}}{\tilde{\rho}} g$. The initial and boundary conditions are

$$\hat{u}(x_0,0) = 0, \qquad \frac{\partial \hat{u}}{\partial t}(x_0,0) = 0, \tag{6.21}$$

$$\hat{u}(0,t) = 0, \qquad E\frac{\partial \hat{u}}{\partial x_0}(H,t) = p_0. \tag{6.22}$$

As derived in Appendix B, the non-homogeneous damped wave equation has the analytical solution

$$\begin{aligned} u(x,t) &= \frac{1}{2}\frac{\tilde{\rho}\tilde{g}}{E}x^2 + \frac{p_0 - \tilde{\rho}\tilde{g}H}{E}x \\ &+ \sum_{n=1}^{\infty} I_{D_n>0}\, u_n \left[\frac{1}{\sqrt{D_n}}\left(-\frac{\rho_w g}{2\tilde{\rho}k} + \frac{\sqrt{D_n}}{2}\right)e^{-\frac{\sqrt{D_n}t}{2}} - \frac{1}{\sqrt{D_n}}\left(-\frac{\rho_w g}{2\tilde{\rho}k} - \frac{\sqrt{D_n}}{2}\right)e^{\frac{\sqrt{D_n}t}{2}}\right] e^{-\frac{\rho_w g t}{2\tilde{\rho}k}} \sin\frac{(2n-1)\pi x}{2H} \\ &+ \sum_{n=1}^{\infty} I_{D_n=0}\, u_n \left[1 + \frac{\rho_w g t}{2\tilde{\rho}k}\right] e^{-\frac{\rho_w g t}{2\tilde{\rho}k}} \sin\frac{(2n-1)\pi x}{2H} \\ &+ \sum_{n=1}^{\infty} I_{D_n<0}\, u_n \left[\cos\frac{\sqrt{-D_n}t}{2} + \frac{1}{\sqrt{-D_n}}\frac{\rho_w g}{\tilde{\rho}k}\sin\frac{\sqrt{-D_n}t}{2}\right] e^{-\frac{\rho_w g t}{2\tilde{\rho}k}} \sin\frac{(2n-1)\pi x}{2H} \end{aligned} \tag{6.23}$$

with coefficients

$$u_n = \frac{8\left(2\pi p_0 n(-1)^n + 2\tilde{\rho}\tilde{g}H - \pi p_0(-1)^n\right)H}{\left(4n^2 - 4n + 1\right)(2n-1)\pi^3 E} \tag{6.24}$$

and discriminants

$$D_n = \left(\frac{\rho_w g}{\tilde{\rho}k}\right)^2 - 4\left(\frac{(2n-1)\pi}{2H}\right)^2 \frac{E}{\tilde{\rho}}. \tag{6.25}$$

In Figure 6.2 the analytical solution of the oedometric deformation $x(t)$ of a porous, saturated medium is plotted for 4 different values of x_0. The used exemplary parameters are listed in the same figure. Only the first 5 terms of the infinite sums are taken into account. Other terms are negligibly small.

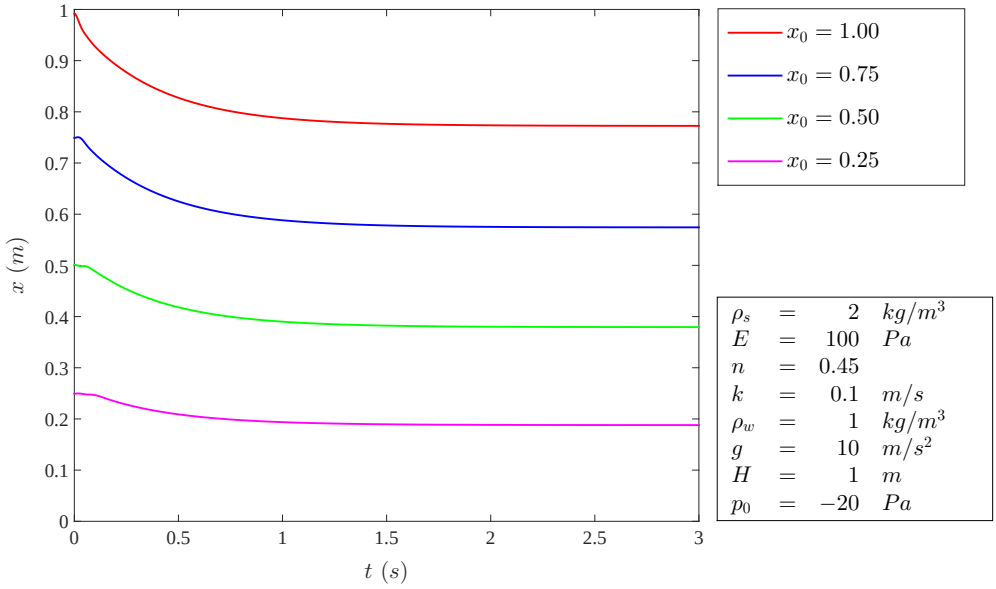

Figure 6.2: Analytical solution for the one dimensional oedometer problem with exemplary parameters

7

FINITE ELEMENT SPACE DISCRETIZATION

This chapter introduces the finite element method for the one dimensional simplified deformation problem given in Section 6.3. The equations are repeated here for convenience

$$\begin{aligned} \tilde{\rho}\frac{\partial \hat{v}}{\partial t} + \frac{\rho_w g}{k}\hat{v} &= \frac{\partial \hat{\sigma}'}{\partial x_0} - \bar{\rho} g, \\ \frac{\partial \hat{\sigma}'}{\partial t} &= E\frac{d\hat{v}}{dx_0}, \\ \frac{\partial \hat{u}}{\partial t} &= \hat{v}, \end{aligned} \tag{7.1}$$

with initial conditions

$$\hat{v}(x_0,0) = 0, \quad \hat{\sigma}(x_0,0) = 0, \quad \hat{u}(x_0,0) = 0, \tag{7.2}$$

and boundary conditions

$$\hat{v}(0,t) = 0, \quad \hat{\sigma}(H,t) = p_0. \tag{7.3}$$

The same procedure as in Chapter 2 is followed. This means that we start with deriving the virtual work equation in Section 7.1. In Section 7.2 this equation is discretized and the corresponding global and element matrices can be found. The chapter ends with an overview of the resulting system of ordinary differential equations in Section 7.3.

7.1. VIRTUAL WORK EQUATION

Let us first recall the momentum equation for the soil-water mixture, after applying all assumptions

$$\tilde{\rho}\frac{\partial \hat{v}}{\partial t} + \frac{\rho_w g}{k}\hat{v} = \frac{\partial \hat{\sigma}'}{\partial x_0} - \bar{\rho} g. \tag{7.4}$$

We multiply the momentum equation by a virtual velocity $\delta\hat{v}$ and integrate over the domain $0 < x_0 < H$ in order to obtain the virtual work equation

$$\int_0^H \delta\hat{v}\tilde{\rho}\frac{\partial \hat{v}}{\partial t}dx_0 + \int_0^H \delta\hat{v}\frac{\rho_w g}{k}\hat{v}dx_0 = \int_0^H \delta\hat{v}\frac{\partial \hat{\sigma}'}{\partial x_0}dx_0 - \int_0^H \delta\hat{v}\bar{\rho} g dx_0. \tag{7.5}$$

When applying integration by parts and the boundary conditions $\sigma'(H,t) = p_0$ and $\delta\hat{v}(0,t) = 0$, the virtual work equation becomes

$$\int_0^H \delta\hat{v}\tilde{\rho}\frac{\partial \hat{v}}{\partial t}dx_0 + \int_0^H \delta\hat{v}\frac{\rho_w g}{k}\hat{v}dx_0 = -\int_0^H \frac{\partial(\delta\hat{v})}{\partial x_0}\hat{\sigma}' dx_0 + \delta\hat{v}(H,t)p_0 - \int_0^H \delta\hat{v}\bar{\rho} g dx_0. \tag{7.6}$$

7.2. GLOBAL AND ELEMENT MATRICES OF THE VIRTUAL WORK EQUATION

In Section 2.2 two different shape functions are introduced. In the simplified 2-phase formulation the linear interpolation functions are again used for the velocity and the displacement. The step functions are now used for the effective stress. When all variables in Equation 7.6 are replaced by their discretized variants, the virtual work equation becomes in matrix notation

$$\mathbf{M}\frac{d\mathbf{v}}{dt} + \mathbf{C}\mathbf{v} = -\mathbf{K}^{\sigma}\boldsymbol{\sigma}' + \mathbf{F}^{trac} + \mathbf{F}^{grav}. \tag{7.7}$$

Taking the water phase into account has rendered a new velocity-dependent term involving matrix $\mathbf{C}$. It can be considered as a damping force, and the matrix $\mathbf{C}$ is therefore referred to as the damping matrix.

The corresponding element matrices and vectors are approximated using Gaussian quadrature with a single Gauss point, see Appendix C.1, after applying the coordinate transformation given by Equation 2.19

$$\begin{aligned}
\mathbf{M}_e &= \int_{x_i}^{x_{i+1}} \mathbf{N}_e^T \tilde{\rho} \mathbf{N}_e dx_0 = \begin{bmatrix} \frac{1}{4}\tilde{\rho}\Delta x_0 & \frac{1}{4}\tilde{\rho}\Delta x_0 \\ \frac{1}{4}\tilde{\rho}\Delta x_0 & \frac{1}{4}\tilde{\rho}\Delta x_0 \end{bmatrix} \\
\mathbf{C}_e &= \int_{x_i}^{x_{i+1}} \mathbf{N}_e^T \frac{\rho_w g}{k} \mathbf{N}_e dx_0 = \begin{bmatrix} \frac{1}{4}\frac{\rho_w g \Delta x_0}{k} & \frac{1}{4}\frac{\rho_w g \Delta x_0}{k} \\ \frac{1}{4}\frac{\rho_w g \Delta x_0}{k} & \frac{1}{4}\frac{\rho_w g \Delta x_0}{k} \end{bmatrix} \\
\mathbf{K}_e^{\sigma} &= \int_{x_i}^{x_{i+1}} \left(\frac{d\mathbf{N}_e}{dx_0}\right)^T \mathbf{K}_e dx_0 = \begin{bmatrix} -1 \\ 1 \end{bmatrix} \\
\mathbf{F}_e^{grav} &= -\int_{x_i}^{x_{i+1}} \mathbf{N}_e^T \bar{\rho} g dx_0 = \begin{bmatrix} -\frac{1}{2}\bar{\rho} g \Delta x_0 \\ -\frac{1}{2}\bar{\rho} g \Delta x_0 \end{bmatrix}
\end{aligned} \tag{7.8}$$

We assume that the reader is now familiar to the assemblage procedure described in Appendix C.2 and immediately give the global matrices and vectors

$$\mathbf{M} = \begin{bmatrix} \frac{1}{4}\tilde{\rho}\Delta x_0 & \frac{1}{4}\tilde{\rho}\Delta x_0 & & & 0 \\ \frac{1}{4}\tilde{\rho}\Delta x_0 & \frac{1}{2}\tilde{\rho}\Delta x_0 & \ddots & & \\ & \ddots & \ddots & \ddots & \\ & & \ddots & \frac{1}{2}\tilde{\rho}\Delta x_0 & \frac{1}{4}\tilde{\rho}\Delta x_0 \\ 0 & & & \frac{1}{4}\tilde{\rho}\Delta x_0 & \frac{1}{4}\tilde{\rho}\Delta x_0 \end{bmatrix} \tag{7.9}$$

$$\mathbf{C} = \begin{bmatrix} \frac{1}{4}\frac{\rho_w g \Delta x_0}{k} & \frac{1}{4}\frac{\rho_w g \Delta x_0}{k} & & & 0 \\ \frac{1}{4}\frac{\rho_w g \Delta x_0}{k} & \frac{1}{2}\frac{\rho_w g \Delta x_0}{k} & \ddots & & \\ & \ddots & \ddots & \ddots & \\ & & \ddots & \frac{1}{2}\frac{\rho_w g \Delta x_0}{k} & \frac{1}{4}\frac{\rho_w g \Delta x_0}{k} \\ 0 & & & \frac{1}{4}\frac{\rho_w g \Delta x_0}{k} & \frac{1}{4}\frac{\rho_w g \Delta x_0}{k} \end{bmatrix} \tag{7.10}$$

$$\mathbf{K}^{\sigma} = \begin{bmatrix} -1 & & & 0 \\ 1 & -1 & & \\ & \ddots & \ddots & \\ & & 1 & -1 \\ 0 & & & 1 \end{bmatrix} \quad \mathbf{F}^{trac} = \begin{bmatrix} 0 \\ 0 \\ \vdots \\ 0 \\ p_0 \end{bmatrix} \quad \mathbf{F}^{grav} = \begin{bmatrix} -\frac{1}{2}\bar{\rho} g \Delta x_0 \\ -\bar{\rho} g \Delta x_0 \\ \vdots \\ -\bar{\rho} g \Delta x_0 \\ -\frac{1}{2}\bar{\rho} g \Delta x_0 \end{bmatrix} \tag{7.11}$$

The lumped mass matrix is again constructed from the mass matrix confirm the lumping procedure in Appendix C.3

$$\mathbf{M}^{L} \approx \begin{bmatrix} \frac{1}{2}\tilde{\rho}\Delta x_0 & & & 0 \\ & \tilde{\rho}\Delta x_0 & & \\ & & \ddots & \\ & & & \frac{1}{2}\tilde{\rho}\Delta x_0 \end{bmatrix}. \tag{7.12}$$

Whether it is necessary to lump the damping matrix $\mathbf{C}$, depends on the time integration scheme. With an implicit method lumping is recommended, while it is better to stick with the more accurate non-lumped damping matrix when considering an explicit method.

7.3. RESULTING SYSTEM OF ORDINARY DIFFERENTIAL EQUATIONS

We conclude this chapter with the system of ordinary differential equations

$$\begin{aligned} \mathbf{M}^{L}\frac{d\mathbf{v}}{dt} + \mathbf{C}\mathbf{v} &= -\mathbf{K}^{\sigma}\boldsymbol{\sigma}' + \mathbf{F}^{trac} + \mathbf{F}^{grav}, \\ \frac{d\boldsymbol{\sigma}'}{dt} &= \mathbf{K}^{v}\mathbf{v}, \\ \frac{d\mathbf{u}}{dt} &= \mathbf{v}, \end{aligned} \tag{7.13}$$

with initial conditions

$$\mathbf{v}(0) = \mathbf{0}, \quad \boldsymbol{\sigma}'(0) = \mathbf{0}, \quad \mathbf{u}(0) = \mathbf{0}. \tag{7.14}$$

In order to be complete we also state the global matrix $\mathbf{K}^{v}$ and element matrices $\mathbf{K}^{v}_{e}$

$$\mathbf{K}^{v} = \begin{bmatrix} -\frac{E}{\Delta x_0} & \frac{E}{\Delta x_0} & & 0 \\ & \ddots & \ddots & \\ & & \ddots & \ddots \\ 0 & & -\frac{E}{\Delta x_0} & \frac{E}{\Delta x_0} \end{bmatrix}, \qquad \mathbf{K}^{v}_{e} = \begin{bmatrix} -\frac{E}{\Delta x_0} & \frac{E}{\Delta x_0} \end{bmatrix}. \tag{7.15}$$

8

EULER-CROMER TIME DISCRETIZATION

The Euler-Cromer method is a semi-implicit time discretization method for Hamiltonian equations. In the 1-phase formulation we indeed dealt with Hamiltonian equations, but the damping term in the simplified 2-phase formulation necessitates an extension. The Euler-Cromer time discretization becomes

$$\begin{aligned} x^{n+1} &= x^n + \Delta t f(x^n, y^n, t^n), \\ y^{n+1} &= y^n + \Delta t g(x^{n+1}, t^n). \end{aligned} \tag{8.1}$$

where the explicit Euler method is still applied to the first equation and the implicit Euler method to the second equation. This extension can be found under the name modified Sielecki method [19].

Recall the system of ordinary differential equations from Section 7.3

$$\begin{aligned} \mathbf{M}^L \frac{d\mathbf{v}}{dt} + \mathbf{C}\mathbf{v} &= -\mathbf{K}^\sigma \boldsymbol{\sigma}' + \mathbf{F}^{trac} + \mathbf{F}^{grav}, \\ \frac{d\boldsymbol{\sigma}'}{dt} &= \mathbf{K}^v \mathbf{v}, \\ \frac{d\mathbf{u}}{dt} &= \mathbf{v}, \end{aligned} \tag{8.2}$$

with initial conditions

$$\mathbf{v}(0) = \mathbf{0}, \quad \boldsymbol{\sigma}'(0) = \mathbf{0}, \quad \mathbf{u}(0) = \mathbf{0}. \tag{8.3}$$

Let $\mathbf{v}^n$, $\boldsymbol{\sigma}^n$ and $\mathbf{u}^n$ denote the velocity, effective stress and displacement respectively at time level $t = n\Delta t$. The initial conditions are now given by

$$\mathbf{v}^0 = \mathbf{0}, \quad \boldsymbol{\sigma}^0 = \mathbf{0}, \quad \mathbf{u}^0 = \mathbf{0}. \tag{8.4}$$

Applying the extended Euler-Cromer time discretization to the first two equations of Equation 8.2 the velocity and effective stress on the next time level can be computed with

$$\begin{aligned} \mathbf{v}^{n+1} &= \mathbf{v}^n + \Delta t \left(\mathbf{M}^L\right)^{-1} \left[-\mathbf{C}\mathbf{v}^n - \mathbf{K}^\sigma \boldsymbol{\sigma}^n + \mathbf{F}^{trac} + \mathbf{F}^{grav} \right], \\ \boldsymbol{\sigma}^{n+1} &= \boldsymbol{\sigma}^n + \Delta t \mathbf{K}^v \mathbf{v}^{n+1} \end{aligned} \tag{8.5}$$

It should be noted that in the explicit expression the consistent damping matrix $\mathbf{C}$ is used.

For the displacement an implicit expression is used

$$\mathbf{u}^{n+1} = \mathbf{u}^n + \Delta t \mathbf{v}^{n+1}. \tag{8.6}$$

The flowchart in Figure 8.1 summarizes the complete solution procedure.

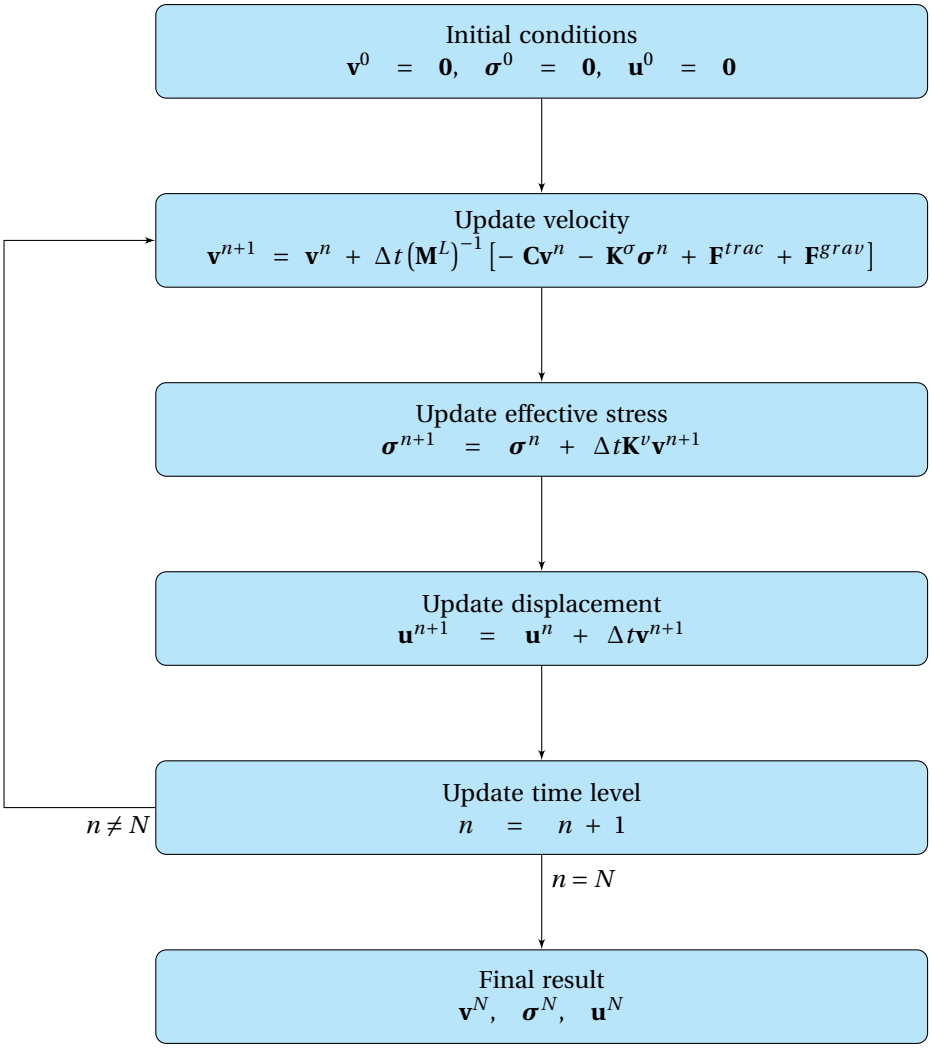

Figure 8.1: Time step procedure for time interval $[0, N\Delta t]$

9

STABILITY ANALYSIS

This chapter contains a detailed stability analysis for the simplified 2-phase formulation of Equation 6.18. The stability analysis considers the finite element space discretization presented in Chapter 7 and the modified Euler-Cromer time discretization presented in Chapter 8.

Similar to the stability analysis of the 1-phase formulation, the analysis is performed using both the Von Neumann method and the matrix method, in Section 9.1 and 9.2, respectively.

9.1. VON NEUMANN METHOD

The Von Neumann method starts with the set of discrete equations derived in Chapter 8, repeated here

$$\begin{aligned} \mathbf{v}^{n+1} &= \mathbf{v}^n + \Delta t \left(\mathbf{M}^L\right)^{-1} \left[-\mathbf{C}\mathbf{v}^n - \mathbf{K}^\sigma \boldsymbol{\sigma}^n + \mathbf{F}^{trac} + \mathbf{F}^{grav} \right], \\ \boldsymbol{\sigma}^{n+1} &= \boldsymbol{\sigma}^n + \Delta t \mathbf{K}^v \mathbf{v}^{n+1} \\ \mathbf{u}^{n+1} &= \mathbf{u}^n + \Delta t \mathbf{v}^{n+1}. \end{aligned} \tag{9.1}$$

Since the method does not take boundary conditions into account, we consider only the change of velocity and displacement of internal node i and the change of stress within element i

$$\begin{aligned} v_i^{n+1} &= v_i^n - \frac{\rho_w g \Delta t}{\tilde{\rho} k} \left(\frac{1}{4} D^{-1} + \frac{1}{2} + \frac{1}{4} D \right) v_i^n + \frac{\Delta t}{\tilde{\rho} \Delta x_0} \left(1 - D^{-1}\right) \sigma_i^n - \frac{\tilde{\rho} \Delta t g}{\tilde{\rho}}, \\ \sigma_i^{n+1} &= \sigma_i^n + \frac{E \Delta t}{\Delta x_0} \left(D - 1\right) v_i^{n+1}, \\ u_i^{n+1} &= u_i^n + \Delta t v_i^{n+1}, \end{aligned} \tag{9.2}$$

where D is the displacement operator introduced in Section 4.1.

In operator form Equations 9.2 become

$$\mathbf{A}(D)\mathbf{x}_i^{n+1} = \mathbf{B}(D)\mathbf{x}_i^n + \mathbf{q} \tag{9.3}$$

with on the left hand side

$$\mathbf{A}(D) = \begin{bmatrix} 1 & 0 & 0 \\ \frac{E\Delta t}{\Delta x_0}(1 - D) & 1 & 0 \\ -\Delta t & 0 & 1 \end{bmatrix} \quad \text{and} \quad \mathbf{x}_i^{n+1} = \begin{bmatrix} v_i^{n+1} \\ \sigma_i^{n+1} \\ u_i^{n+1} \end{bmatrix}, \tag{9.4}$$

and on the right hand side

$$\mathbf{B}(D) = \begin{bmatrix} 1 - \frac{\rho_w g \Delta t}{\tilde{\rho} k}\left(\frac{1}{4}D^{-1} + \frac{1}{2} + \frac{1}{4}D\right) & \frac{\Delta t}{\tilde{\rho}\Delta x_0}\left(1 - D^{-1}\right) & 0 \\ 0 & 1 & 0 \\ 0 & 0 & 1 \end{bmatrix}, \quad \mathbf{x}_i^n = \begin{bmatrix} v_i^n \\ \sigma_i^n \\ u_i^n \end{bmatrix} \quad \text{and} \quad \mathbf{q} = \begin{bmatrix} -\frac{\tilde{\rho}\Delta t g}{\tilde{\rho}} \\ 0 \\ 0 \end{bmatrix}. \tag{9.5}$$

We know that performing the Von Neumann method is equivalent to solving the eigenvalue problem in Equation 4.15, given by

$$\mathbf{B}\left(e^{I\phi}\right)\mathbf{v} = \lambda \mathbf{A}\left(e^{I\phi}\right)\mathbf{v}. \tag{9.6}$$

The characteristic equation corresponding to Equation 9.6 is

$$(1-\lambda)\left[\lambda^2 + (c + 4d - 2)\lambda + (1 - c)\right] = 0 \tag{9.7}$$

with

$$c = \frac{\rho_w g \Delta t}{\tilde{\rho} k}\cos^2\left(\frac{\phi}{2}\right) \quad \text{and} \quad d = \frac{E\Delta t^2}{\tilde{\rho}\Delta x_0^2}\sin^2\left(\frac{\phi}{2}\right). \tag{9.8}$$

The eigenvalues are then computed as the roots of the characteristic equation

$$\lambda_1 = 1, \qquad \lambda_{2,3} = 1 - \frac{1}{2}c - 2d \pm \sqrt{(1 - \frac{1}{2}c - 2d)^2 - (1 - c)}, \tag{9.9}$$

The Von Neumann stability criterion then renders

$$\left|1 - \frac{1}{2}c - 2d \pm \sqrt{(1 - \frac{1}{2}c - 2d)^2 - (1 - c)}\right| \leq 1, \qquad \text{for all } \phi \in [-\pi, \pi]. \tag{9.10}$$

which can be simplified using Lemma 4.1

$$-2 + c \leq 2 - c - 4d \leq 2 - c \quad \text{and} \quad 1 - c \leq 1, \qquad \text{for all } \phi \in [-\pi, \pi], \tag{9.11}$$

or equivalently

$$c \geq 0, \quad d \geq 0 \quad \text{and} \quad c + 2d \leq 2, \qquad \text{for all } \phi \in [-\pi, \pi]. \tag{9.12}$$

Replacing c and d by Equations 9.8 results in the final expression

$$0 \leq \frac{\rho_w g \Delta t}{\tilde{\rho} k} \leq 2 \quad \text{and} \quad 0 \leq \frac{E\Delta t^2}{\tilde{\rho}\Delta x_0^2} \leq 1, \tag{9.13}$$

and gives critical time step

$$\Delta t_{crit} = \min\left(\frac{2\tilde{\rho} k}{\rho_w g}, \frac{\Delta x_0}{\sqrt{E/\tilde{\rho}}}\right) \tag{9.14}$$

Compared to the stability criterion of the 1-phase formulation, we see that there is an extra criterion that needs to be satisfied in the simplified 2-phase formulation. This extra criterion does not depend on the mesh but is purely based on material properties, specifically the hydraulic conductivity k.

9.2. MATRIX METHOD

For the matrix method we start with the set of ordinary differential equations from Section 7.3 given by

$$\begin{aligned} \mathbf{M}^L \frac{d\mathbf{v}}{dt} + \mathbf{C}\mathbf{v} &= -\mathbf{K}^\sigma \boldsymbol{\sigma} + \mathbf{F}^{trac} + \mathbf{F}^{grav}, \\ \frac{d\boldsymbol{\sigma}}{dt} &= \mathbf{K}^v \mathbf{v}, \\ \frac{d\mathbf{u}}{dt} &= \mathbf{v}. \end{aligned} \tag{9.15}$$

We transform these equations into one second order ordinary differential equation

$$\mathbf{M}^L \frac{d^2\mathbf{u}}{dt^2} + \mathbf{C}\frac{d\mathbf{u}}{dt} = -\mathbf{K}^\sigma \mathbf{K}^\nu \mathbf{u} + \mathbf{F}^{trac} + \mathbf{F}^{grav} \tag{9.16}$$

with error equation

$$\mathbf{M}^L \frac{d^2\boldsymbol{\eta}}{dt^2} + \mathbf{C}\frac{d\boldsymbol{\eta}}{dt} = -\mathbf{K}^\sigma \mathbf{K}^\nu \boldsymbol{\eta}. \tag{9.17}$$

First note that the damping matrix $\mathbf{C}$ is a linear combination of the lumped mass matrix $\mathbf{M}^L$ and the stiffness matrix $\mathbf{K}^\sigma\mathbf{K}^\nu$

$$\mathbf{C} = a_1\mathbf{M}^L + a_2\mathbf{K}^\sigma\mathbf{K}^\nu \tag{9.18}$$

with

$$a_1 = \frac{\rho_w g}{\tilde{\rho} k} \quad \text{and} \quad a_2 = -\frac{\rho_w g \Delta x_0^2}{4Ek}. \tag{9.19}$$

Equation 9.17 then becomes

$$\mathbf{M}^L \frac{d^2\boldsymbol{\epsilon}}{dt^2} + a_1\mathbf{M}^L\frac{d\boldsymbol{\epsilon}}{dt} = -a_2\mathbf{K}^\sigma\mathbf{K}^\nu\frac{d\boldsymbol{\epsilon}}{dt} - \mathbf{K}^\sigma\mathbf{K}^\nu\boldsymbol{\epsilon}. \tag{9.20}$$

Now the problem can be uncoupled by solving the eigenvalue problem

$$\mathbf{K}^\sigma\mathbf{K}^\nu\mathbf{v} = \lambda\mathbf{M}^L\mathbf{v}. \tag{9.21}$$

Since a similar eigenvalue problem is solved in Section 4.2, we may copy the result with a slight adaptation of the parameters

$$0 \le \lambda \le \frac{4E}{\tilde{\rho}\Delta x_0^2}. \tag{9.22}$$

We are now able to reconsider Equation 9.20 as

$$\frac{d^2\boldsymbol{\eta}}{dt^2} + (a_1 + a_2\lambda)\frac{d\boldsymbol{\eta}}{dt} = -\lambda\boldsymbol{\eta}. \tag{9.23}$$

or componentwise

$$\frac{d^2\eta_j}{dt^2} + (a_1 + a_2\lambda)\frac{d\eta_j}{dt} = -\lambda\eta_j, \tag{9.24}$$

when $\boldsymbol{\eta}$ expresses the eigenvector corresponding to eigenvalue λ.

This second order differential equation is equivalent to the system of first order differential equations

$$\begin{aligned} \frac{d\eta_{j1}}{dt} &= -(a_1 + a_2\lambda)\eta_{j1} - \lambda\eta_{j2}, \\ \frac{d\eta_{j2}}{dt} &= \eta_{j1}, \end{aligned} \tag{9.25}$$

to which we apply the modified Euler-Cromer method as described in Chapter 8

$$\begin{aligned} \eta_{j1}^{n+1} &= \eta_{j1}^n - \Delta t(a_1 + a_2\lambda)\eta_{j1}^n - \Delta t\lambda\epsilon_{j2}^n, \\ \eta_{j2}^{n+1} &= \eta_{j2}^n + \Delta t\eta_{j1}^{n+1}. \end{aligned} \tag{9.26}$$

In matrix notation this becomes

$$\begin{bmatrix} 1 & 0 \\ -\Delta t & 1 \end{bmatrix} \begin{bmatrix} \eta_{j1}^{n+1} \\ \eta_{j2}^{n+1} \end{bmatrix} = \begin{bmatrix} 1-\Delta t(a_1+a_2\lambda) & -\lambda\Delta t \\ 0 & 1 \end{bmatrix} \begin{bmatrix} \eta_{j1}^{n} \\ \eta_{j2}^{n} \end{bmatrix} \tag{9.27}$$

The eigenvalues μ belonging to its corresponding eigenvalue problem equal

$$\begin{aligned}\mu_{1,2} &= 1 - \frac{1}{2}\lambda\Delta t^2 - \frac{1}{2}a_1\Delta t - \frac{1}{2}a_2\lambda\Delta t \\ &\pm \sqrt{\left(1 - \frac{1}{2}\lambda\Delta t^2 - \frac{1}{2}a_1\Delta t - \frac{1}{2}a_2\lambda\Delta t\right)^2 - (1 - a_1\Delta t - a_2\lambda\Delta t)}\end{aligned} \tag{9.28}$$

Lemma 4.1 replaces the criterion $|\mu_{1,2}| \leq 1$ by

$$-2 + a_1\Delta t + a_2\lambda\Delta t \leq 2 - \lambda\Delta t^2 - a_1\Delta t - a_2\lambda\Delta t \leq 2 - a_1\Delta t - a_2\lambda\Delta t \tag{9.29}$$

and

$$1 - a_1\Delta t - a_2\lambda\Delta t \leq 1. \tag{9.30}$$

These equation are equivalent to

$$\lambda\Delta t^2 \geq 0, \qquad a_1\Delta t + a_2\lambda\Delta t \geq 0 \qquad \text{and} \qquad \lambda\Delta t^2 + 2a_1\Delta t + 2a_2\lambda\Delta t \leq 4. \tag{9.31}$$

Replacing a_1 and a_2 by Equations 9.19 gives

$$0 \leq \lambda \leq \frac{4E}{\tilde{\rho}\Delta x_0^2} \qquad \text{and} \qquad \left(\Delta t^2 - \frac{\rho_w g \Delta x_0^2 \Delta t}{2Ek}\right)\lambda + \frac{2\rho_w g\Delta t}{\tilde{\rho}k} \leq 4. \tag{9.32}$$

Taking into account the estimate for λ in Equation 9.22, this is satisfied when

$$0 \leq \frac{\rho_w g \Delta t}{\tilde{\rho}k} \leq 2 \qquad \text{and} \qquad 0 \leq \frac{E\Delta t^2}{\tilde{\rho}\Delta x_0^2} \leq 1. \tag{9.33}$$

The critical time step equals

$$\Delta t_{crit} = \min\left(\frac{2\tilde{\rho}k}{\rho_w g}, \frac{\Delta x_0}{\sqrt{E/\tilde{\rho}}}\right) \tag{9.34}$$

Both the Von Neumann and matrix method give the same stability criterion.

10

VALIDATION OF OBTAINED STABILITY CRITERIA

For the validation of the time step criteria of the simplified 2-phase formulation, the formulation is implemented in Matlab regarding the finite element space discretization of Chapter 7 and the Euler-Cromer time discretization of Chapter 8. Chapter 9 shows that the corresponding time step criteria lead to a critical time step

$$0 \leq \frac{\rho_w g \Delta t}{\tilde{\rho} k} \leq 2 \quad \text{and} \quad 0 \leq \frac{E \Delta t^2}{\tilde{\rho} \Delta x_0^2} \leq 1 \quad \longrightarrow \quad \Delta t_{crit} = \min\left(\frac{2\tilde{\rho} k}{\rho_w g}, \frac{\Delta x_0}{\sqrt{E/\tilde{\rho}}} \right) \tag{10.1}$$

The validation of the time step criterion will therefore consist of two steps.

ρ_s	$=$	2	kg/m^3	g	$=$	10	m/s^2
E	$=$	100	Pa	p_0	$=$	-20	Pa
n	$=$	0.45		H	$=$	1	m
ρ_w	$=$	1	kg/m^3	Δx_0	$=$	0.01	m

Table 10.1: List of examplary parameters

Let us first consider the parameters given in Table 10.1. Some investigation tells us that with a high hydraulic conductivity $k = 0.1\ m/s$ the mesh-dependent criterion determines the critical time step

$$k = 0.1\ m/s \quad \longrightarrow \quad \frac{2\tilde{\rho} k}{\rho_w g} = 0.03544\ s, \ \frac{\Delta x_0}{\sqrt{E/\tilde{\rho}}} = 0.00133\ s \quad \longrightarrow \quad \Delta t_{crit} = 0.00133\ s. \tag{10.2}$$

In Figure 10.1 both the numerical solutions and analytical solutions are plotted with a time step that is slightly smaller than the critical time step. The numerical method is clearly stable, since the numerical solutions coincide with the corresponding analytical solutions. Figure 10.2 shows that the numerical method is unstable with a time step slightly larger than the critical time step. These two figures therefore confirm the correctness of the mesh-dependent criterion.

The other inequality can be checked considering the parameters in Table 10.1 in combination with a low hydraulic conductivity

$$k = 0.001\ m/s \quad \longrightarrow \quad \frac{2\tilde{\rho} k}{\rho_w g} = 0.000354\ s, \ \frac{\Delta x_0}{\sqrt{E/\tilde{\rho}}} = 0.00133\ s \quad \longrightarrow \quad \Delta t_{crit} = 0.000354\ s. \tag{10.3}$$

Now Figure 10.3 and 10.4 show respectively the stable and unstable numerical method with time steps that lie around the critical time step, which means that also the mesh-independent criterion is validated.

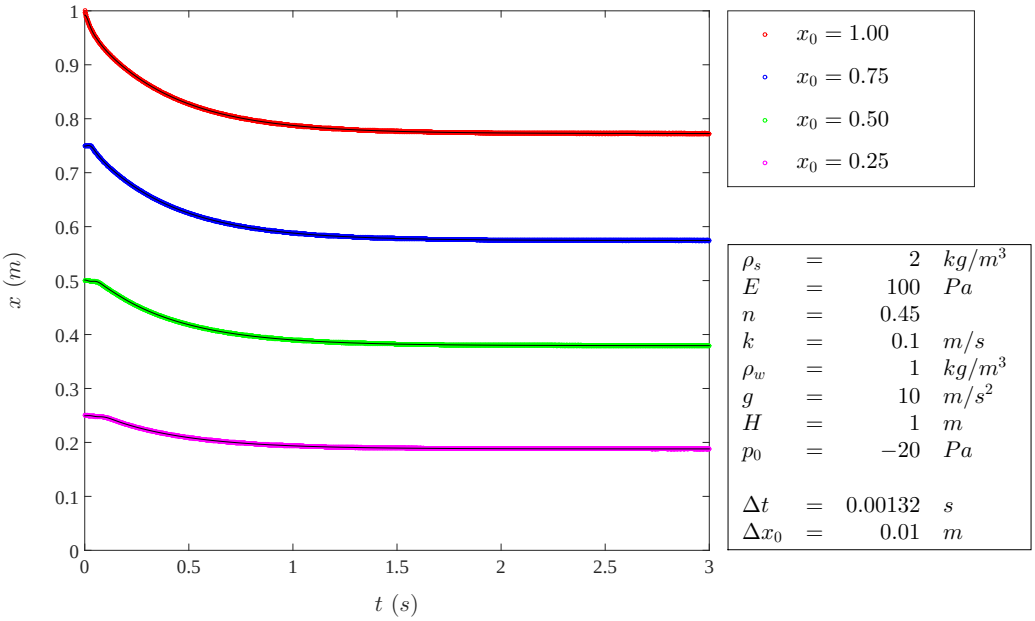

Figure 10.1: Comparison of numerical and analytical solution for 1D oedometer problem for $k = 0,1 \; m/s$ and $\Delta t = 0,99 \Delta t_{crit}$, rendering stable numerical analysis

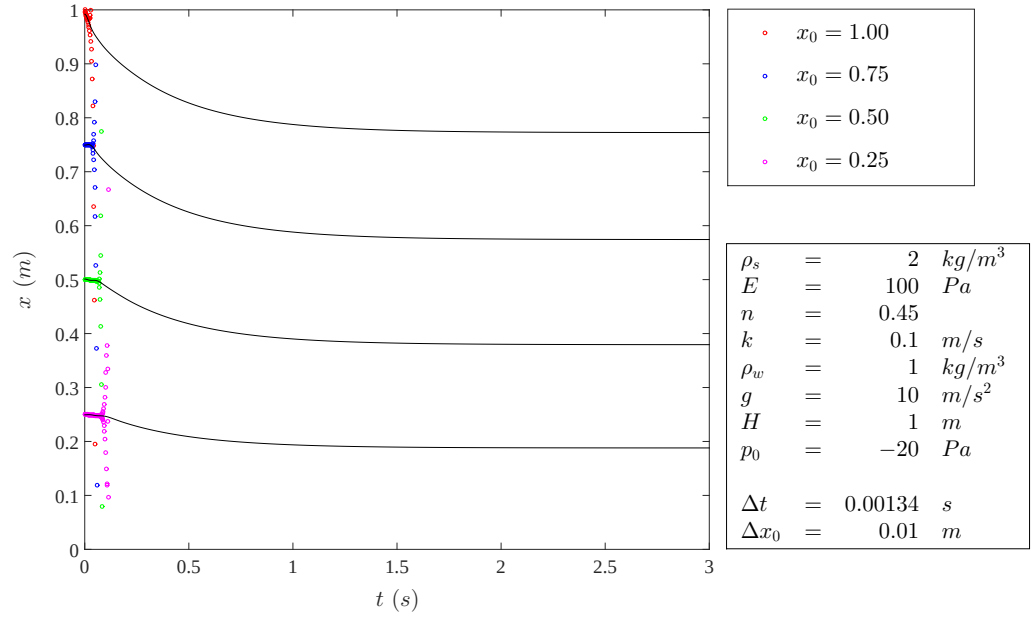

Figure 10.2: Comparison of numerical and analytical solution for 1D oedometer problem for $k = 0,1 \; m/s$ and $\Delta t = 1,01 \Delta t_{crit}$, rendering unstable numerical analysis

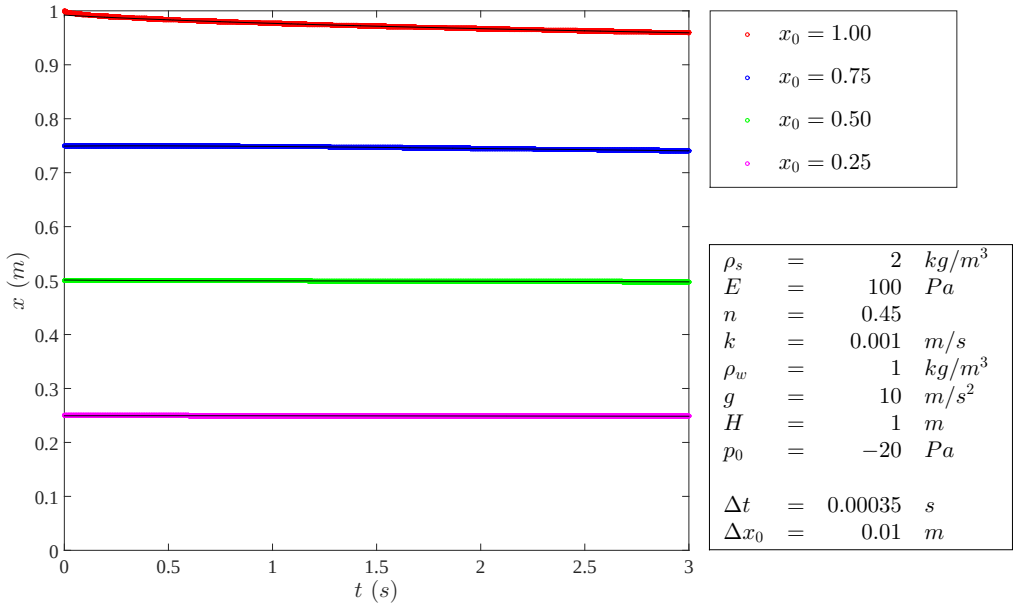

Figure 10.3: Comparison of numerical and analytical solution for 1D oedometer problem for $k = 0,001 \; m/s$ and $\Delta t = 0,99 \Delta t_{crit}$, rendering stable numerical analysis

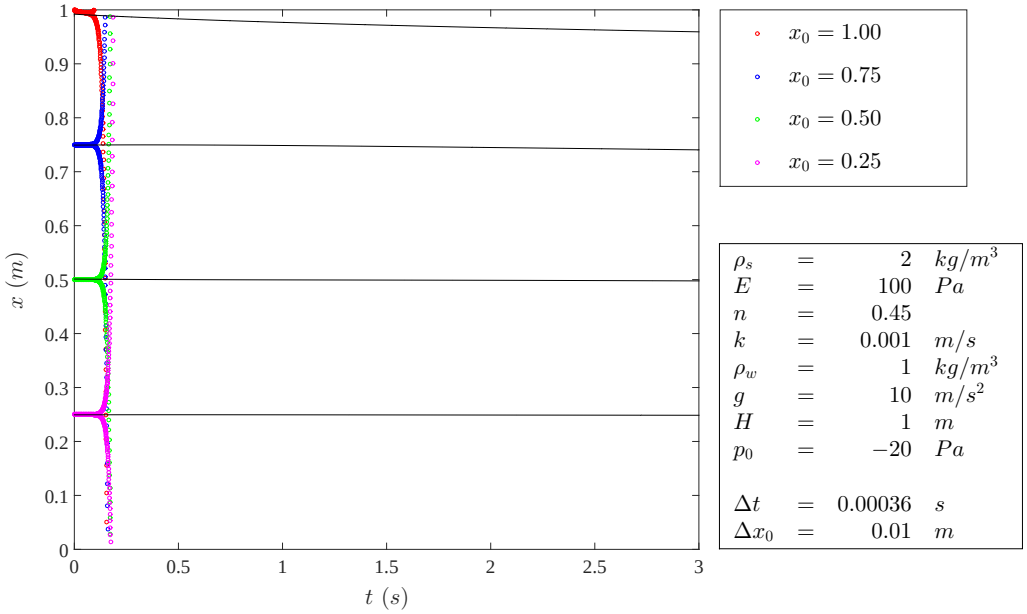

Figure 10.4: Comparison of numerical and analytical solution for 1D oedometer problem for $k = 0,001 \; m/s$ and $\Delta t = 1,01 \Delta t_{crit}$, rendering stable numerical analysis

CONCLUDING REMARKS

The goal of this thesis is to determine a stability criterion for the Euler-Cromer method applied to analyses of consolidation with the finite element method as well as the material point method. Three dimensional dynamic problems are considered involving, in case of analyses with the material point method, large deformations of soil. A velocity-based 2-phase formulation is used to describe the time-dependent deformation of water-saturated soil upon loading. The complexity of the underlying physical model is further increased when taking into consideration the highly non-linear deformation behaviour of soil.

In this thesis, the complexity of the physical model is increased in steps. In this preliminary study soil was first considered as a 1-phase continuum of a linear-elastic material. Finite Element space discretization and Euler-Cromer time discretization were applied to a one dimensional case, an oedometer test.
Subsequent stability analyses with both the Von Neumann and matrix method require solving challenging eigenvalue problems. With the help of Lemma 4.1 the analyses could be greatly simplified. The analyses rendered the well-known critical time step

$$\Delta t_{crit} = \frac{\Delta x}{\sqrt{E/\rho}}$$

thus proving the validity of the approach.

In the second part of this preliminary study the liquid phase was taken into account. Since a stability analysis for the full 2-phase formulation still poses a challenging problem for the one dimensional case, the assumption of an incompressible liquid phase was introduced to obtain a simplified formulation.
The Von Neumann method and matrix method now showed that the presence of a damping term in the equation of motion renders a second time step criterion. The two obtained criteria read

$$\frac{E\Delta t^2}{\tilde{\rho}\Delta x^2} \leq 1 \quad \text{and} \quad \frac{\rho_w g \Delta t}{\tilde{\rho} k} \leq 2,$$

rendering the critical time step

$$\Delta t_{crit} = \min\left(\frac{\Delta x}{\sqrt{E/\tilde{\rho}}}, \frac{2\tilde{\rho}k}{\rho_w g}\right).$$

It has been validated for the one dimensional case.

It can be concluded from this preliminary study that the liquid phase, the hydraulic conductivity respectively, influence the numerical stability of the Euler-Cromer scheme applied to the simplified 2-phase formulation.

In the course of this thesis, the study will be extended to the full 2-phase formulation and to the three dimensional case. Here, the effects of mesh boundary and artificial local damping will be investigated. It is expected that results can be applied to analyses involving geometric and material non-linearity too, when the critical time step size is recomputed after each time step. This would allow to apply the formulation enhanced by a stability criterion to three dimensional geotechnical problems such as cone penetration testing or slope failure.

A

ANALYTICAL SOLUTION TO NON-HOMOGENEOUS WAVE EQUATION

Consider the following non-homogeneous wave equation with initial and boundary conditions

$$\begin{cases} \frac{\partial^2 u}{\partial t^2} = \frac{E}{\rho}\frac{\partial^2 u}{\partial x^2} - g, & 0 < x < H,\ t > 0 \\ u(x,0) = 0, & \frac{\partial u}{\partial t}(x,0) = 0, \\ u(0,t) = 0, & E\frac{\partial u}{\partial x}(H,t) = p_0. \end{cases} \tag{A.1}$$

Let us first find the equilibrium solution $u_E(x)$, that satisfies

$$\begin{cases} 0 = \frac{E}{\rho}\frac{\partial^2 u_E}{\partial x^2} - g, & 0 < x < H \\ u_E(0) = 0, & E\frac{\partial u_E}{\partial x}(H) = p_0. \end{cases} \tag{A.2}$$

Integrating the differential equation twice results in

$$u_E(x) = \frac{1}{2}\frac{\rho g}{E}x^2 + a_1 x + a_2. \tag{A.3}$$

The two boundary conditions then determine the two integration constants

$$u_E(0) = a_2 = 0 \longrightarrow a_2 = 0 \tag{A.4}$$

$$E\frac{\partial u_E}{\partial x}(H) = \rho g H + E a_1 = p_0 \longrightarrow a_1 = \frac{p_0 - \rho g H}{E}, \tag{A.5}$$

which yields the following equilibrium solution

$$u_E(x) = \frac{1}{2}\frac{\rho g}{E}x^2 + \frac{p_0 - \rho g H}{E}x. \tag{A.6}$$

Assume now that the solution to the wave equation is a superposition of the equilibrium solution u_E and an unknown function v

$$u(x,t) = u_E(x) + v(x,t). \tag{A.7}$$

Then we can deduce that the unknown function v should satisfy:

$$\begin{cases} \frac{\partial^2 v}{\partial t^2} = \frac{E}{\rho}\frac{\partial^2 v}{\partial x^2}, & 0 < x < H,\ t > 0 \\ v(x,0) = -u_E(x), & \frac{\partial v}{\partial t}(x,0) = 0, \\ v(0,t) = 0, & \frac{\partial v}{\partial x}(H,t) = 0. \end{cases} \tag{A.8}$$

This partial differential equation can be solved using the method of seperation of variables, where $v(x,t) = \phi(x)G(t)$. The partial differential equation can then be rearranged and set equal to a separation constant, that Haberman [20] proved to be real

$$\phi(x)\frac{d^2G}{dt^2}(t) = \frac{E}{\rho}\frac{d^2\phi}{dx^2}(x)G(t) \longrightarrow \frac{\rho}{EG(t)}\frac{d^2G}{dt^2} = \frac{1}{\phi(x)}\frac{d^2\phi}{dx^2} = -\lambda. \tag{A.9}$$

This results in two ordinary differential equations, from which we first consider the spatial differential equation

$$\frac{d^2\phi}{dx^2} = -\lambda\phi. \tag{A.10}$$

Boundary conditions for $\phi(x)$ follow from the boundary conditions for $v(x,t)$

$$\phi(0)G(t) = 0,\ \frac{d\phi}{dx}(H)G(t) = 0 \longrightarrow \phi(0) = 0,\ \frac{d\phi}{dx}(H) = 0. \tag{A.11}$$

Note that $G(t) = 0$ is not considered, since we are interested in a non-trivial solution.

When $\lambda > 0$ the solution is the sum of a cosinus and a sinus

$$\phi(x) = b_1\cos\sqrt{\lambda}x + b_2\sin\sqrt{\lambda}x \tag{A.12}$$

In order to satisfy the boundary condition $\phi(0) = 0$, we find $b_1 = 0$. The other boundary condition then yields

$$b_2\sqrt{\lambda}\cos\sqrt{\lambda}H = 0 \tag{A.13}$$

The coefficient b_2 should be nonzero in order to imply a non-trivial solution, so the only possibilities are

$$\lambda = \left(\frac{(2n-1)\pi}{2H}\right)^2, \quad \text{for } n = 1,2,3,\ldots \tag{A.14}$$

with associated functions

$$\phi(x) = b_2\sin\frac{(2n-1)\pi x}{2H}, \quad \text{for } n = 1,2,3,\ldots \tag{A.15}$$

When $\lambda = 0$ the solution is a linear polynomial

$$\phi(x) = c_1x + c_2 \tag{A.16}$$

but the boundary conditions imply the trivial solution.

When $\lambda < 0$ the solution is the sum of a cosinus hyperbolicus and sinus hyperbolicus:

$$\phi(x) = d_1\cosh\sqrt{-\lambda}x + d_2\sinh\sqrt{-\lambda}x \tag{A.17}$$

but the boundary conditions again imply the trivial solution.

In conclusion the boundary value problem has only positive eigenvalues

$$\lambda = \left(\frac{(2n-1)\pi}{2H}\right)^2, \quad \text{for } n = 1,2,3,\ldots \tag{A.18}$$

with corresponding eigenfunctions

$$\phi(x) = b_2\sin\frac{(2n-1)\pi x}{2H}, \quad \text{for } n = 1,2,3,\ldots \tag{A.19}$$

The time-dependent differential equation equals

$$\frac{d^2G}{dt^2} = -\lambda\frac{E}{\rho}G. \tag{A.20}$$

and has general solution

$$G(t) = e_1 \cos\sqrt{\frac{E}{\rho}}\frac{(2n-1)\pi t}{2H} + e_2 \sin\sqrt{\frac{E}{\rho}}\frac{(2n-1)\pi t}{2H}, \qquad \text{for } n = 1,2,3,\ldots \tag{A.21}$$

Combining both $\phi(x)$ and $G(t)$ for all allowable λ the solution becomes

$$v(x,t) = \sum_{n=1}^{\infty}\left(f_n \cos\sqrt{\frac{E}{\rho}}\frac{(2n-1)\pi t}{2H} + g_n \sin\sqrt{\frac{E}{\rho}}\frac{(2n-1)\pi t}{2H}\right)\sin\frac{(2n-1)\pi x}{2H}, \tag{A.22}$$

The final step in the derivation is finding the unknowns f_n and g_n with help of the initial conditions

$$\sum_{n=1}^{\infty} f_n \sin\frac{(2n-1)\pi x}{2H} = -u_E(x), \tag{A.23}$$

$$\sum_{n=1}^{\infty} g_n \sqrt{\frac{E}{\rho}}\frac{(2n-1)\pi}{2H}\sin\frac{(2n-1)\pi x}{2H} = 0 \tag{A.24}$$

By orthogonality of the sines the first initial condition results in

$$f_n = \frac{-\int_0^H u_E(x)\sin\frac{(2n-1)\pi x}{2H}dx}{\int_0^H \sin^2\frac{(2n-1)\pi x}{2H}dx} = \frac{8\left(2\pi p_0 n(-1)^n + 2\rho g H - \pi p_0(-1)^n\right)H}{\left(4n^2-4n+1\right)(2n-1)\pi^3 E}, \qquad \text{for } n = 1,2,3,\ldots \tag{A.25}$$

The second initial condition implies

$$g_n = 0, \qquad \text{for } n = 1,2,3,\ldots \tag{A.26}$$

The unknown function v is therewith determined

$$v(x,t) = \sum_{n=1}^{\infty}\frac{8\left(2\pi p_0 n(-1)^n + 2\rho g H - \pi p_0(-1)^n\right)H}{\left(4n^2-4n+1\right)(2n-1)\pi^3 E}\cos\sqrt{\frac{E}{\rho}}\frac{(2n-1)\pi t}{2H}\sin\frac{(2n-1)\pi x}{2H}, \tag{A.27}$$

The solution to the non-homogeneous wave equation with initial and boundary condition then becomes

$$u(x,t) = \frac{1}{2}\frac{\rho g}{E}x^2 + \frac{p_0 - \rho g H}{E}x + \sum_{n=1}^{\infty} u_n \cos\sqrt{\frac{E}{\rho}}\frac{(2n-1)\pi t}{2H}\sin\frac{(2n-1)\pi x}{2H}, \tag{A.28}$$

$$u_n = \frac{8\left(2\pi p_0 n(-1)^n + 2\rho g H - \pi p_0(-1)^n\right)H}{\left(4n^2-4n+1\right)(2n-1)\pi^3 E} \tag{A.29}$$

B

ANALYTICAL SOLUTION TO NON-HOMOGENEOUS DAMPED WAVE EQUATION

Consider the following non-homogeneous damped wave equation with initial and boundary conditions

$$\begin{cases} \frac{\partial^2 u}{\partial t^2} + \frac{\rho_w g}{\tilde{\rho} k}\frac{\partial u}{\partial t} = \frac{E}{\tilde{\rho}}\frac{\partial^2 u}{\partial x^2} - \tilde{g}, & 0 < x < H,\ t > 0 \\ u(x,0) = 0, & \frac{\partial u}{\partial t}(x,0) = 0, \\ u(0,t) = 0, & E\frac{\partial u}{\partial x}(H,t) = p_0. \end{cases} \tag{B.1}$$

Let us first find the equilibrium solution $u_E(x)$, that satisfies

$$\begin{cases} 0 = \frac{E}{\tilde{\rho}}\frac{\partial^2 u_E}{\partial x^2} - \tilde{g}, & 0 < x < H \\ u_E(0) = 0, & E\frac{\partial u_E}{\partial x}(H) = p_0. \end{cases} \tag{B.2}$$

From appendix A we know that the equilibrium equation has the following solution, taking notice of the slightly different parameters

$$u_E(x) = \frac{1}{2}\frac{\tilde{\rho}\tilde{g}}{E}x^2 + \frac{p_0 - \tilde{\rho}\tilde{g}H}{E}x. \tag{B.3}$$

Assume now that the solution to the wave equation is a superposition of the equilibrium solution u_E and an unknown function v

$$u(x,t) = u_E(x) + v(x,t). \tag{B.4}$$

Then we can deduce that the unknown function v should satisfy

$$\begin{cases} \frac{\partial^2 v}{\partial t^2} + \frac{\rho_w g}{\tilde{\rho} k}\frac{\partial v}{\partial t} = \frac{E}{\tilde{\rho}}\frac{\partial^2 v}{\partial x^2}, & 0 < x < H,\ t > 0 \\ v(x,0) = -u_E(x), & \frac{\partial v}{\partial t}(x,0) = 0, \\ v(0,t) = 0, & \frac{\partial v}{\partial x}(H,t) = 0. \end{cases} \tag{B.5}$$

This partial differential equation can be solved using the method of seperation of variables, where $v(x,t) = \phi(x)G(t)$. The partial differential equation can then be rearranged and set equal to a separation constant, that Haberman [20] proved to be real

$$\phi\frac{d^2G}{dt^2} + \frac{\rho_w g}{\tilde{\rho} k}\phi\frac{dG}{dt} = \frac{E}{\tilde{\rho}}\frac{d^2\phi}{dx^2}G \quad \longrightarrow \quad \frac{\tilde{\rho}}{EG}\left[\frac{d^2G}{dt^2} + \frac{\rho_w g}{\tilde{\rho} k}\frac{dG}{dt}\right] = \frac{1}{\phi}\frac{d^2\phi}{dx^2} = -\lambda. \tag{B.6}$$

This results in two ordinary differential equations, from which we first consider the spatial differential equation

$$\frac{d^2\phi}{dx^2} = -\lambda\phi. \tag{B.7}$$

According to appendix A the only non-trivial solutions that satisfy the boundary conditions $\phi(0) = 0$ and $\frac{d\phi}{dx}(H) = 0$ are positive eigenvalues

$$\lambda = \left(\frac{(2n-1)\pi}{2H}\right)^2, \qquad \text{for } n = 1,2,3,\ldots \tag{B.8}$$

with corresponding eigenfunctions

$$\phi(x) = b_2 \sin\frac{(2n-1)\pi x}{2H}, \qquad \text{for } n = 1,2,3,\ldots \tag{B.9}$$

For the eigenvalue $\lambda = \left(\frac{(2n-1)\pi}{2H}\right)^2$ the time-dependent differential equation equals

$$\frac{d^2G}{dt^2} + \frac{\rho_w g}{\tilde{\rho}k}\frac{dG}{dt} = -\left(\frac{(2n-1)\pi}{2H}\right)^2 \frac{E}{\tilde{\rho}}G. \tag{B.10}$$

The shape of the solution depends on the discriminant belonging to this problem

$$D_n = \left(\frac{\rho_w g}{\tilde{\rho}k}\right)^2 - 4\left(\frac{(2n-1)\pi}{2H}\right)^2 \frac{E}{\tilde{\rho}} \tag{B.11}$$

For $D_n > 0$ the solution to the differential equation equals

$$G(t) = \left[e_1 e^{-\frac{\sqrt{D_n}t}{2}} + e_2 e^{\frac{\sqrt{D_n}t}{2}}\right] e^{-\frac{\rho_w g t}{2\tilde{\rho}k}} \tag{B.12}$$

For $D_n = 0$ the solution to the differential equation equals

$$G(t) = [e_1 + e_2 t]\, e^{-\frac{\rho_w g t}{2\tilde{\rho}k}} \tag{B.13}$$

And finally, for $D_n < 0$ the solution to the differential equation equals

$$G(t) = \left[e_1 \cos\frac{\sqrt{-D_n}t}{2} + e_2 \sin\frac{\sqrt{-D_n}t}{2}\right] e^{-\frac{\rho_w g t}{2\tilde{\rho}k}} \tag{B.14}$$

Combining both $\phi(x)$ and $G(t)$ for all allowable λ the solution becomes

$$\begin{aligned} v(x,t) = &\sum_{n=1}^{\infty} I_{D_n>0}\left[f_n e^{-\frac{\sqrt{D_n}t}{2}} + g_n e^{\frac{\sqrt{D_n}t}{2}}\right] e^{-\frac{\rho_w g t}{2\tilde{\rho}k}} \sin\frac{(2n-1)\pi x}{2H} \\ &+ \sum_{n=1}^{\infty} I_{D_n=0}\left[f_n + g_n t\right] e^{-\frac{\rho_w g t}{2\tilde{\rho}k}} \sin\frac{(2n-1)\pi x}{2H} \\ &+ \sum_{n=1}^{\infty} I_{D_n<0}\left[f_n \cos\frac{\sqrt{-D_n}t}{2} + g_n \sin\frac{\sqrt{-D_n}t}{2}\right] e^{-\frac{\rho_w g t}{2\tilde{\rho}k}} \sin\frac{(2n-1)\pi x}{2H} \end{aligned} \tag{B.15}$$

where $I_A = 1$ if statement A is true and $I_A = 0$ if statement A is false.

The final step in the derivation is finding the unknowns f_n and g_n with help of the initial conditions

$$\begin{aligned} &\sum_{n=1}^{\infty} I_{D_n>0}\left[f_n + g_n\right] \sin\frac{(2n-1)\pi x}{2H} \\ &\quad + \sum_{n=1}^{\infty} I_{D_n=0} f_n \sin\frac{(2n-1)\pi x}{2H} \\ &\quad + \sum_{n=1}^{\infty} I_{D_n<0} f_n \sin\frac{(2n-1)\pi x}{2H} = -u_E(x), \end{aligned} \tag{B.16}$$

and

$$\sum_{n=1}^{\infty} I_{D_n>0}\left[\left(-\frac{\rho_w g}{2\tilde{\rho}k}-\frac{\sqrt{D_n}}{2}\right)f_n+\left(-\frac{\rho_w g}{2\tilde{\rho}k}+\frac{\sqrt{D_n}}{2}\right)g_n\right]\sin\frac{(2n-1)\pi x}{2H} + \sum_{n=1}^{\infty} I_{D_n=0}\left[-\frac{\rho_w g}{2\tilde{\rho}k}f_n+g_n\right]\sin\frac{(2n-1)\pi x}{2H} + \sum_{n=1}^{\infty} I_{D_n<0}\left[-\frac{\rho_w g}{2\tilde{\rho}k}f_n+\frac{\sqrt{-D_n}}{2}g_n\right]\sin\frac{(2n-1)\pi x}{2H} = 0. \quad \text{(B.17)}$$

Using a similar approach as in appendix A, the initial conditions result in

$$I_{D_n>0}\left[f_n+g_n\right]+I_{D_n=0}f_n+I_{D_n<0}f_n = \frac{8\left(2\pi p_0 n(-1)^n+2\tilde{\rho}\tilde{g}H-\pi p_0(-1)^n\right)H}{\left(4n^2-4n+1\right)(2n-1)\pi^3 E}, \quad \text{(B.18)}$$

and

$$I_{D_n>0}\left[\left(-\frac{\rho_w g}{2\tilde{\rho}k}-\frac{\sqrt{D_n}}{2}\right)f_n+\left(-\frac{\rho_w g}{2\tilde{\rho}k}+\frac{\sqrt{D_n}}{2}\right)g_n\right] + I_{D_n=0}\left[-\frac{\rho_w g}{2\tilde{\rho}k}f_n+g_n\right]+I_{D_n<0}\left[-\frac{\rho_w g}{2\tilde{\rho}k}f_n+\frac{\sqrt{-D_n}}{2}g_n\right] = 0, \quad \text{(B.19)}$$

for $n = 1,2,3,\ldots$.

Filtering all f_n and g_n gives the unknown function v

$$\begin{aligned} v(x,t) = & \sum_{n=1}^{\infty} I_{D_n>0}v_n\left[\frac{1}{\sqrt{D_n}}\left(-\frac{\rho_w g}{2\tilde{\rho}k}+\frac{\sqrt{D_n}}{2}\right)e^{-\frac{\sqrt{D_n}t}{2}}-\frac{1}{\sqrt{D_n}}\left(-\frac{\rho_w g}{2\tilde{\rho}k}-\frac{\sqrt{D_n}}{2}\right)e^{\frac{\sqrt{D_n}t}{2}}\right]e^{-\frac{\rho_w g t}{2\tilde{\rho}k}}\sin\frac{(2n-1)\pi x}{2H} \\ & + \sum_{n=1}^{\infty} I_{D_n=0}v_n\left[1+\frac{\rho_w g t}{2\tilde{\rho}k}\right]e^{-\frac{\rho_w g t}{2\tilde{\rho}k}}\sin\frac{(2n-1)\pi x}{2H} \\ & + \sum_{n=1}^{\infty} I_{D_n<0}v_n\left[\cos\frac{\sqrt{-D_n}t}{2}+\frac{1}{\sqrt{-D_n}}\frac{\rho_w g}{\tilde{\rho}k}\sin\frac{\sqrt{-D_n}t}{2}\right]e^{-\frac{\rho_w g t}{2\tilde{\rho}k}}\sin\frac{(2n-1)\pi x}{2H} \end{aligned} \quad \text{(B.20)}$$

where

$$v_n = \frac{8\left(2\pi p_0 n(-1)^n+2\tilde{\rho}\tilde{g}H-\pi p_0(-1)^n\right)H}{\left(4n^2-4n+1\right)(2n-1)\pi^3 E} \quad \text{(B.21)}$$

The solution to the non-homogeneous damped wave equation with initial and boundary condition then becomes

$$\begin{aligned} u(x,t) = & \frac{1}{2}\frac{\tilde{\rho}\tilde{g}}{E}x^2+\frac{p_0-\tilde{\rho}\tilde{g}H}{E}x \\ & + \sum_{n=1}^{\infty} I_{D_n>0}u_n\left[\frac{1}{\sqrt{D_n}}\left(-\frac{\rho_w g}{2\tilde{\rho}k}+\frac{\sqrt{D_n}}{2}\right)e^{-\frac{\sqrt{D_n}t}{2}}-\frac{1}{\sqrt{D_n}}\left(-\frac{\rho_w g}{2\tilde{\rho}k}-\frac{\sqrt{D_n}}{2}\right)e^{\frac{\sqrt{D_n}t}{2}}\right]e^{-\frac{\rho_w g t}{2\tilde{\rho}k}}\sin\frac{(2n-1)\pi x}{2H} \\ & + \sum_{n=1}^{\infty} I_{D_n=0}u_n\left[1+\frac{\rho_w g t}{2\tilde{\rho}k}\right]e^{-\frac{\rho_w g t}{2\tilde{\rho}k}}\sin\frac{(2n-1)\pi x}{2H} \\ & + \sum_{n=1}^{\infty} I_{D_n<0}u_n\left[\cos\frac{\sqrt{-D_n}t}{2}+\frac{1}{\sqrt{-D_n}}\frac{\rho_w g}{\tilde{\rho}k}\sin\frac{\sqrt{-D_n}t}{2}\right]e^{-\frac{\rho_w g t}{2\tilde{\rho}k}}\sin\frac{(2n-1)\pi x}{2H} \end{aligned} \quad \text{(B.22)}$$

where

$$u_n = \frac{8\left(2\pi p_0 n(-1)^n+2\tilde{\rho}\tilde{g}H-\pi p_0(-1)^n\right)H}{\left(4n^2-4n+1\right)(2n-1)\pi^3 E} \quad \text{(B.23)}$$

C

MATHEMATICAL TECHNIQUES

This Appendix introduces several mathematical techniques that are used during this thesis: Gaussian quadrature in Section C.1 to integrate numerically, the assemblage procedure in Section C.2 to assemble global matrices (vectors) from element matrices (vectors) and the lumping procedure in Section C.3 to construct diagonal matrices from non-diagonal matricess.

C.1. GAUSSIAN QUADRATURE IN ONE DIMENSION

Consider a line segment $[a,b]$ illustrated in Figure C.1 and a function $g(x)$. Gaussian quadrature is an approximation method that uses n Gauss points to approximate the integral of $g(x)$ over the line segment:

$$\int_{\Omega} g(\xi)d\Omega \approx \sum_{q=1}^{n} \omega_q g(\xi_q) \tag{C.1}$$

with weight ω_q and position ξ_q for each Gauss point. Note that Gaussian quadrature with n Gauss points is exact for polynomials up to order n.

Figure C.1: Line element $[a,b]$

In case of a single Gauss point we calculate its weight ω_q and coordinate x_q by assuming that Gaussian quadrature is exact for polynomials up to order one

$$\int_a^b dx = b-a = \omega_q \quad \rightarrow \quad \omega_q = b-a \tag{C.2}$$

$$\int_a^b x\,dx = \frac{1}{2}(b-a)^2 = \omega_q x_q \quad \rightarrow \quad x_q = \frac{1}{2}(b-a) \tag{C.3}$$

The location of the Gauss point is exactly in the middle of the line element, see Figure C.2.

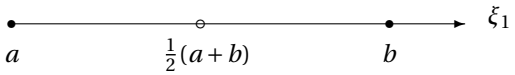

Figure C.2: Single Gauss point in line element $[a,b]$

C.2. ASSEMBLAGE PROCEDURE

For a global matrix $\mathbf{A}$ (vector $\mathbf{F}$) and corresponding element matrices $\mathbf{A}_e$ (vectors $\mathbf{F}_e$) the assemblage procedure can be written as

$$\mathbf{A} = \sum_{e=1}^{n_e} \mathbf{B}_e^T \mathbf{A}_e \mathbf{B}_e \qquad \left(\mathbf{F} = \sum_{e=1}^{n_e} \mathbf{B}_e^T \mathbf{F}_e \mathbf{B}_e \right), \tag{C.4}$$

with matrix $\mathbf{B}_e$ a boolean matrix that maps a global vector into a vector associated with element e [21].

As an example we consider the three line elements in Figure C.3.

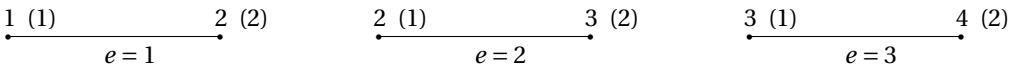

Figure C.3: Three line elements with global and local node numbers

From the global and local node numbers we can derive the boolean matrices $\mathbf{B}_e$

$$\mathbf{B}_1 = \begin{bmatrix} 1 & 0 & 0 & 0 \\ 0 & 1 & 0 & 0 \end{bmatrix}, \quad \mathbf{B}_2 = \begin{bmatrix} 0 & 1 & 0 & 0 \\ 0 & 0 & 1 & 0 \end{bmatrix}, \quad \mathbf{B}_3 = \begin{bmatrix} 0 & 0 & 1 & 0 \\ 0 & 0 & 0 & 1 \end{bmatrix}. \tag{C.5}$$

When the element matrices $\mathbf{A}_e$ equal

$$\mathbf{A}_1 = \begin{bmatrix} 1 & 1 \\ 1 & 1 \end{bmatrix}, \quad \mathbf{A}_2 = \begin{bmatrix} 2 & 2 \\ 2 & 2 \end{bmatrix}, \quad \mathbf{A}_3 = \begin{bmatrix} 3 & 3 \\ 3 & 3 \end{bmatrix}, \tag{C.6}$$

then the global matrix $\mathbf{A}$ is contructed with the assemblage procedure

$$\mathbf{A} = \begin{bmatrix} 1 & 1 & 0 & 0 \\ 1 & 3 & 2 & 0 \\ 0 & 2 & 5 & 3 \\ 0 & 0 & 3 & 3 \end{bmatrix}. \tag{C.7}$$

C.3. LUMPING PROCEDURE

With the lumping procedure diagonal matrix is constructed from a non-diagonal matrix. The diagonal and the non-diagonal matrix are denoted as the lumped matrix $\mathbf{A}^L$ and the full matrix $\mathbf{A}$ respectively. Each diagonal entry of the lumped matrix equals the row sum of the full matrix

$$A_{ii}^L = \sum_{j=1}^{n} A_{ij}. \tag{C.8}$$

Consider for example the following full matrix

$$A = \begin{bmatrix} 4 & 0 & 1 & 1 \\ 2 & 9 & 1 & 0 \\ 0 & 1 & 3 & 0 \\ 1 & 2 & 0 & 5 \end{bmatrix}. \tag{C.9}$$

Applying the lumping procedure results in the following lumped matrix

$$A^L = \begin{bmatrix} 6 & 0 & 0 & 0 \\ 0 & 12 & 0 & 0 \\ 0 & 0 & 4 & 0 \\ 0 & 0 & 0 & 8 \end{bmatrix}. \tag{C.10}$$

D

Proof of Lemma 4.1

Lemma 4.1. *Let a, b be real numbers that satisfy the inequality*

$$\left|a \pm \sqrt{a^2 - b}\right| \leq 1. \tag{D.1}$$

Then a, b satisfy

$$-1 - b \leq 2a \leq 1 + b \quad \text{and} \quad b \leq 1. \tag{D.2}$$

Proof. The proof of this lemma consists of three steps.

1) Assume $a^2 < b$, such that $\sqrt{a^2 - b}$ is complex-valued. Then Equation D.1 implies

$$\left|a \pm \sqrt{a^2 - b}\right|^2 = \left|a \pm i\sqrt{b - a^2}\right|^2 = a^2 + b - a^2 = b \leq 1. \tag{D.3}$$

2) Assume $a^2 = b$, such that $\sqrt{a^2 - b} = 0$. Then Equation D.1 implies

$$-1 \leq a \pm \sqrt{a^2 - b} = a \leq 1. \tag{D.4}$$

3) Assume $a^2 > b$, such that $\sqrt{a^2 - b}$ is real-valued. Then Equation D.1 implies

$$-1 \leq a + \sqrt{a^2 - b} \leq 1 \quad \text{and} \quad -1 \leq a - \sqrt{a^2 - b} \leq 1. \tag{D.5}$$

The sum of these inequalities renders

$$-1 \leq a \leq 1. \tag{D.6}$$

These are consistent with

$$-1 \leq a + \sqrt{a^2 - b} \quad \text{and} \quad a - \sqrt{a^2 - b} \leq 1. \tag{D.7}$$

This leaves us with

$$\begin{aligned} a + \sqrt{a^2 - b} &\leq 1 \\ \sqrt{a^2 - b} &\leq 1 - a \\ a^2 - b &\leq 1 - 2a + a^2 \\ 2a &\leq 1 + b \end{aligned} \tag{D.8}$$

and

$$\begin{aligned} -1 &\leq a - \sqrt{a^2 - b} \\ \sqrt{a^2 - b} &\leq 1 + a \\ a^2 - b &\leq 1 + 2a + a^2 \\ -1 - b &\leq 2a. \end{aligned} \tag{D.9}$$

Combining the three steps renders

$$-1 - b \leq 2a \leq 1 + b \quad \text{and} \quad b \leq 1. \tag{D.10}$$

This is illustrated in Figure D.1, where the parabola represents the equality $a^2 = b$. □

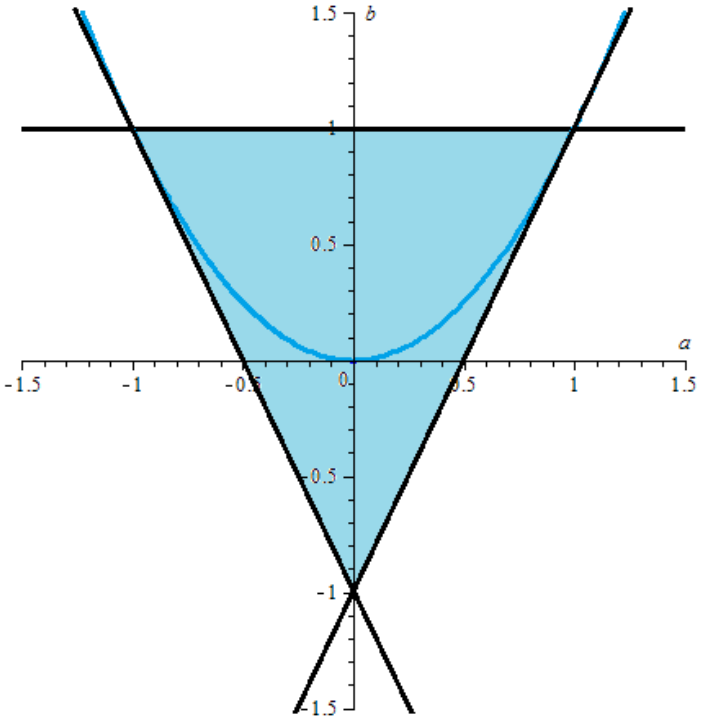

Figure D.1: Area covered by the inequalities $-1-b \leq 2a \leq 1+b$ and $b \leq 1$.

BIBLIOGRAPHY

[1] C. Kenter and P. Vermeer, *Computation by Finite Elements,* in *Foundation Aspects of Coastal Structures* (1978).

[2] B. Van Dijk and F. Kaalberg, *3-D geotechnical model for the North/Southline in Amsterdam,* in *Application of Numerical Methods to Geotechnical Problems* (1998).

[3] I. AL-Kafaji, *Formulation of a Dynamic Material Point Method (MPM) for Geomechanical Problems*, Ph.D. thesis, Institut für Geotechnik der Universität Stuttgart (2013).

[4] K. von Terzaghi, *Erdbaumechanik auf bodenphysikalischer Grundlage* (Deuticke, 1925).

[5] M. Biot, *General Theory of Three-Dimensional Consolidation,* Journal of Applied Physics **12**, p. 155 (1941).

[6] J. Van Esch, D. Stolle, and I. Jassim, *Finite Element Method for Coupled Dynamic Flow-Deformation Simulation,* in *2nd International Symposium on Computational Geomechanics* (2011).

[7] A. Verruijt, *Soil Dynamics* (Delft University of Technology, 2009).

[8] F. Ceccato, *Study of Large Deformation Geomechanical Problems with the Material Point Method*, Ph.D. thesis, Universitá degli Studi di Padova DICEA (2015).

[9] J. Donea, A. Huerta, J.-P. Ponthot, and A. Rodríguez-Ferran, *Arbitrary Lagrangian–Eulerian Methods,* Encyclopedia of Computational Mechanics **1**, p. 413 (2004).

[10] L. Malvern, *Introduction to the Mechanics of a Continuous Medium* (Prentice Hall, 1969).

[11] C. Felippa, *Introduction to Finite Element Methods* (University of Colorado, 2004).

[12] O. Zienkiewicz and R. Taylor, *The Finite Element Method Volume 1: The Basis* (Butterworth-Heinemann, 2000).

[13] A. Cromer, *Stable Solutions using the Euler Approximation,* American Journal of Physics **49**, p. 455 (1981).

[14] C. Hirsch, *Numerical Computation of Internal and External Flows: The Fundamentals of Numerical Discretization* (John Wiley & Sons, 1988).

[15] R. Richtmyer and K. Morton, *Difference Methods for Initial-Value Problems* (John Wiley & Sons, 1967).

[16] B. Irons and S. Ahmad, *Techniques of Finite Elements* (Ellis Horwood, 1980).

[17] R. Courant, K. Friedrichs, and H. Lewy, *Über die partiellen Differenzengleichungen der mathematischen Physik,* Mathematische Annalen **100**, p. 32 (1928).

[18] A. Verruijt, *Soil Mechanics* (Delft University of Technology, 2004).

[19] R. Diependaal, H. Duifhuis, H. Hoogstraten, and M. Viergever, *Numerical Methods for Solving One-Dimensional Cochlear Models in the Time Domain,* Journal of the Acoustical Society of America **82**, p. 1655 (1987).

[20] R. Haberman, *Applied Partial Differential Equations with Fourier Series and Boundary Value Problems* (Prentice Hall, 2004).

[21] D. Loghin, M. van Gijzen, and E. Jonkers, *Bounds on the eigenvalue range and on the field of values of non-Hermitian and indefinite finite element matrices,* Journal of Computational and Applied Mathematics **189**, p. 304 (2006).